ARISTOTLE UNIVERSITY OF THESSALONIKI
FACULTY OF SCIENCES
SCHOOL OF GEOLOGY
DEPARTMENT OF MINERALOGY-PETROLOGY-ECONOMIC GEOLOGY

PRODROMOS I. NIKOLAIDIS

COPPER MINERALIZATION IN RODINGITES FROM ANO GAREFI, ARIDEA AREA, NORTHERN GREECE

B.Sc. thesis

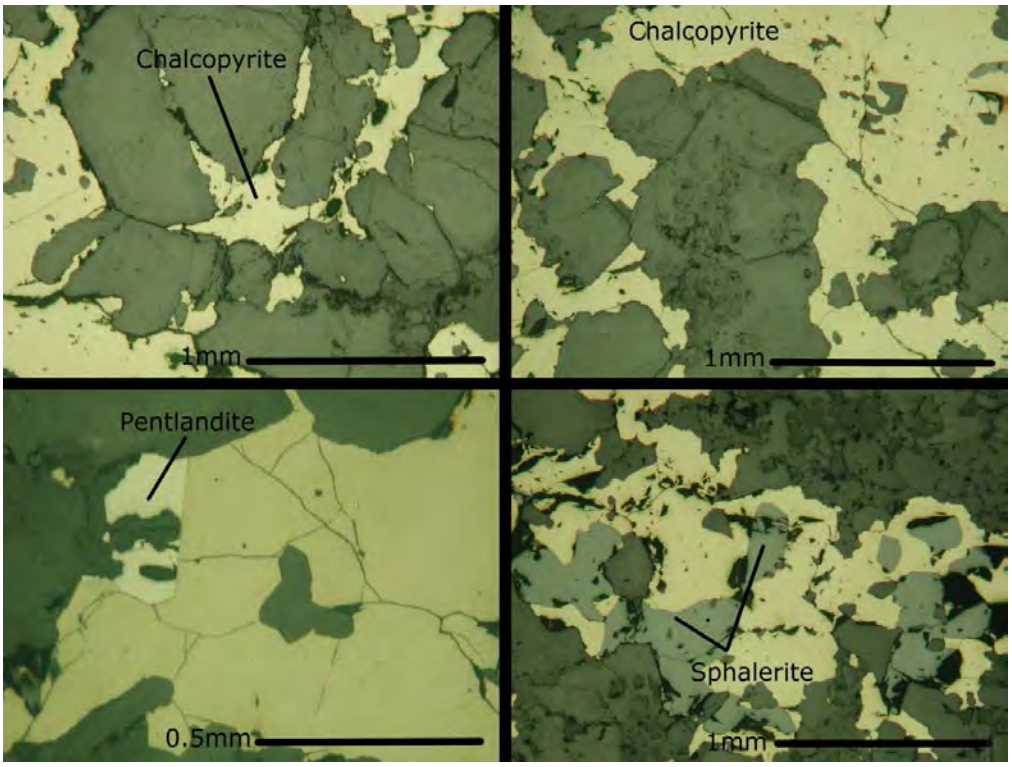

THESSALONIKI
2017

PRODROMOS I. NIKOLAIDIS

COPPER MINERALIZATION IN RODINGITES FROM ANO GAREFI, ARIDEA AREA, NORTHERN GREECE

B.Sc. thesis
Submitted to the School of Geology
Department of Mineralogy-Petrology-Economic Geology
7 Mars 2017

Supervisor Professor
Kleopas M. Michailidis

Examiners
Professor Michail K. Vavelidis
Professor Anestis A. Filippidis
Asst. Professor Vasilios I. Melfos

Contents

1. Abstract

The aim of this B.Sc. thesis was to study the mineral assemblages of the rodingites from Ano Garefi in Aridea area (Northern Greece) and to verify the conditions under which these rocks were formed and in particular to consider the not so common associated copper mineralization in terms of the rodingitization process. The study area is the mountainous terrain above Ano Garefi village which geotectonically belongs to the Almopia subzone of the Axios zone. The Ano Garefi rodingites occur as pods, veins and blocks enclosed in serpentinites and usually adjacent to small or large tectonically included carbonate bodies. Macroscopically, these rodingites have a pale green-brown color while their mineral constituents are medium- to coarse-grained. The identified mineral assemblages consist of calcite + garnet + epidote + clinopyroxene + chlorite ± chromite + chalcopyrite ± pentlandite ± sphalerite. Calcite occurs as local clasts, as veins or even as extended masses enclosing the silicate minerals. Garnets are usually well crystallized and display marked birefringence and anisotropism. A sector zoning and a chemical differentiation from core to rim can be found in most of the garnet crystals. Chemically, they belong to the ugrandite series with andradite as the dominant end-member. The rims of the garnet crystals are usually overgrown by a thin epidote crust. Epidote also forms separate euhedral and prismatic crystals. The clinopyroxenes found within the Ano Garefi rodingites are of diopside-hedenbergite composition. Additionally, wollastonite compositions were found as a result of enrichment in terms of Ca due to the close contact between the rodingites and the carbonate bodies. Chlorite forms small pale green flakes interstitially found to the other minerals and has a pycnochlorite composition. Chromite is a relic mineral of serpentinite protolith and occurs as partly altered to ferritchromite fractured clasts showing evidence of tectonic deformation. The ore minerals, consisting mainly of chalcopyrite with minor pentlandite and sphalerite can be found as local segregations filling the interstices between the gangue minerals. The sulfide mineral content approximately accounts for about 5% by volume of the rodingite body. Chalcopyrite from Ano Garefi has a typical chemical composition with atomic proportions of Cu and Fe, based on 2 S, in the range of 0.824-1.081(mean 0.944) and 0.827-1.040 (mean 0.931), respectively. Pentlandite is a cobaltian variety, with atomic proportions of Co, Fe and Ni, based on 8 S, in the range between 4.912-5.961 (mean 5.312), 0.911-1.580 (mean 1.188) and 1.604-2.682 (mean 2.008), respectively. Sphalerite is characterized by relatively low iron contents. Based on 1 S, Zn ranges between 0.860-0.935 with a mean value of 0.896 while Fe ranges between 0.022-0.054 with a mean value of 0.039. Textural features and mineral associations of the copper bearing rodingites in study, denote that their formation can be attributed to a metasomatic process by means of hydrothermal fluids. These fluids were enriched in the necessary chemical elements by the depletion of the surrounding rocks and circulated through tectonically weakened zones. The reaction zone occurs between carbonate bodies and serpentinites. The carbonate bodies are the main source of Ca while serpentinites are the source of Fe and Mg. Dolerites, associated with the serpentinites, are the most likely source for Al and Cu.

2. Preface

As an undergraduate student very soon I realized that economic geology, which is the science dealing with the discovering, the studying of the formation and the extracting of earth materials that have some economic potential in society, was a very interesting science for me. But what really fascinates me is the first stage of economic geology or in other words the part of exploration geology.

Briefly, an exploration geologist's job is to locate and discover a new ore deposit. To do so, the geologist must firstly clarify and define what kind of an ore deposit is going to look for (e.g. gold, copper, zinc, nickel etc) in a specific and restricted area. The next step is to gather all the available information concerning the area such as previous geoscientific researches, drillhole data, geological maps and schemes, satellite and aerial photos, geophysical data and everything else that might be useful and helpful in the discovering of a new ore deposit. The next step, after collecting all the available information, is to make a quick evaluation and then a general image starts to take shape. At this point, the geologist is called to decide whether the area is favorable to host or not an ore deposit and if it is worth continuing with further research. Further research means that additional information must be collected. In order to acquire new information, the geologist must visit and hike the area, often through rough and adverse conditions. The field investigation, which chronically may vary from days to years, includes the verification of accuracy of older information, drawing a more detailed geological map in a probably larger scale and taking rock or soil samples for chemical analyses and microscope observation. Then comes the hard part, where all this quite different information, which at first glance may seem a little chaotic, after combined together under logical procedures, through a reasonable geological interpretation and a strong geological model might lead to an indication of a probable ore bearing area.

So after all, someone could say that exploration geology is like a modern treasure hunting, where the geologist is called to put all the pieces together in order to find the ore deposit, or in other words the treasure!

Combining my fascination for exploration geology with my love of my broader hometown area was an obvious choice. So, I sought out a B.Sc. thesis, where I could apply some very basic exploration geology techniques as close as possible to my hometown. My final purpose of this work is to gain some experience and knowledge related to my science field and make a very small contribution in understanding the geology of the area.

At this point, I would like to heartfully thank my closest people, standing by me under any circumstances. Special thanks to my supervisor professor, Michailidis Kleopas, for his invaluable guidance and help which he provided me through the writing of this B.Sc. thesis.

3. Introduction

The aim of this B.Sc. thesis was to study the mineral assemblages of the rodingites from Ano Garefi in Aridea area (Northern Greece) and to verify the conditions under which these rocks were formed and in particular to consider the not so common associated copper mineralization in terms of the rodingitization process.

Rodingite is a term firstly used by Bell et al. (1911) to describe igneous dykes of coarse-grained gabbro-like rock that penetrate serpentinites. These investigators in their report assumed that other scientists had already encountered similar rocks in the past according to the descriptions they heard or read, and decided to name them rodingites due to the fact that the most abundant occurrence of these rocks are found in Roding river in Nelson, New Zealand. The decision to name these rocks rodingites was based in the following facts. Firstly, the term gabbro could not be used because it implied the presence of feldspars in the rock but such minerals were not observed. Secondly, the chemical composition showed that the rock was ultrabasic and didn't belong to the basic gabbros while the third and last fact was that the high percentage of calcite and lime in general, completely distinguished it from all other ultrabasic rocks. So after all, it was clear to the investigators that they were dealing with a new rock and thus a new name had to be implied to it.

Since then, rodingites have been spotted in many places throughout the world and studied carefully.

According to Zharikov et al. (2007), the recommended definition of IUGS's subcommission on the systematics of metamorphic rocks is that rodingites are metasomatic rocks primarily composed of grossular-andradite garnet and calcic pyroxene. Vesuvianite, epidote, scapolite and iron ores are characteristic accessory minerals. Rodingites mostly replace dykes or inclusions of basic rocks within serpentinized ultramafic bodies. They may also replace other basic rocks, such as volcanic rocks or amphibolites associated with ultramafic bodies.

A more extended and detailed definition would probably be that rodingites are metasomatized rocks in close relationship with ophiolites due to the fact that they occur as dykes or blocks enclosed in serpentinized peridotite. In outcrop, rodingites are dense lithic formations, which resemble to calcic skarns and hydrothermal vein deposits. Chemical analyses have shown that they are enriched in Ca, alkali-poor, undersaturated in terms of Si (showing an ultrabasic chemical composition) and primarily composed of Ca-Mg and/or Ca-Al silicates such as garnet/hydrogarnet (grossular-andradite), pyroxene (diopside-hedenbergite), epidote, zoisite, clinozoisite, vesuvianite, prehnite, calcite, chlorite and others. The protolith, which will be transformed into rodingite via the metasomatism process, varies chemically from gabbro to quartzite. This means that the protolith rock may as well be for example gabbro, diabase, andesite, granite or even slate (Schandl et al. 1989, O'Hanley 1996, Hatzipanagiotou and Tsikouras 2001, Normand and Williams-Jones 2007, Pomonis et al. 2008).

So briefly, the term rodingite is now referred to any rock type that contains calc-silicate rich mineral assemblages and occurs in contact with serpentinites.

Usually rodingites are barren rocks and the presence of ore minerals is thought to be rare and scarce. However, in some places, like the area studied in this thesis, ore minerals do exist within rodingites. For example, Murzin and Shanina (2007) and Murzin et al. (2009) investigations are study cases of rodingites with ore mineral assemblages.

The study area of this B.Sc. thesis is the mountainous terrain above Ano Garefi village which belongs to the municipality of Aridea in Pella prefecture (Figure 1).

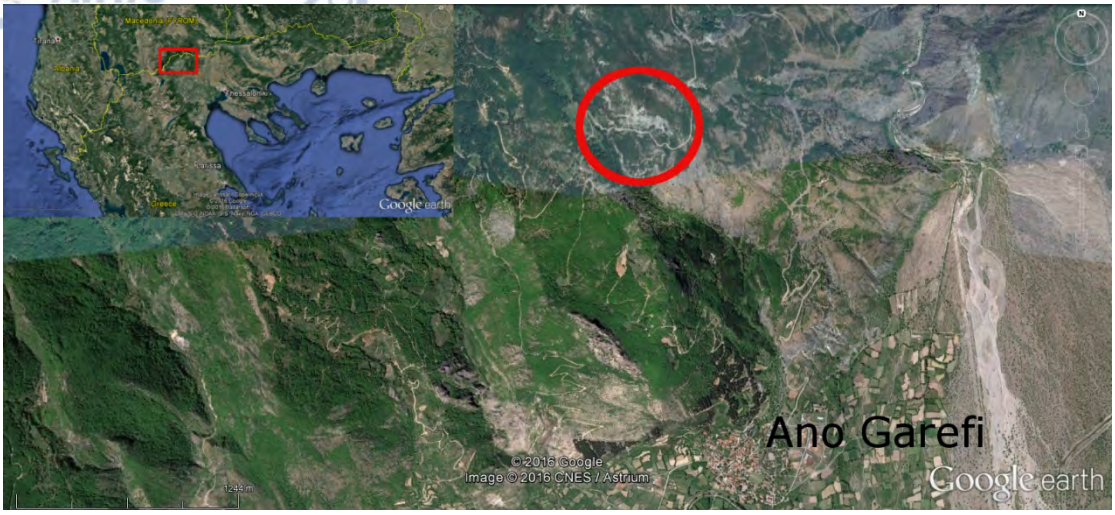

Figure 1: Satellite image of the study area. The main picture is the enlargement of the red rectangle in the reference map taken from an altitude of 6.50km during 2016. The red circle shows the rodingite sampling area (41.051053° latitude, 22.035946°longitude).

The copper bearing rodingites were randomly spotted in 1980 during a field investigation of a different purpose, by the supervisor professor Michailidis Kleopas and his colleagues, near the small chapel of Zoodohos Pighi which is built up in the mountain about 2km northwest (measured in linear distance) of Ano Garefi village.

However, the main mineralization site wasn't discovered for the very first time in 1980. Small historic research, questionable though because it is based on the villagers' stories which were verbally passed down generation after generation, and field evidence such as the existence of an exploration mining gallery are indicative of that and according to this data the age of discovery is thought to be around 1912, during the Balkan wars, when an effort for exploitation by extracting the ore was made.

Back in 1980, samples were collected in order to construct thin and thin-polished sections for microscopy observations. Some mineral analyses were performed but no further research or publication was carried out until now.

The same thin and thin-polished sections were carefully reexamined within this thesis accompanied by new electron probe microanalyses conducted by a Scanning Electron Microscope (SEM).

4. Geological setting

Through time, Greece has been divided by many researchers into some geotectonic zones according to various criteria such as petrology, metamorphism, sedimentation, paleogeography etc. As a result every zone has its unique characteristics, differentiating one from another. It must be pointed out, however, that until this time, the geotectonic zone separation of Greece is not yet in its final form due to the existence of many contradictory opinions from various geoscientists and is constantly subjected to changes as new data come to light. A generally acceptable scheme of this zone separation by Mountrakis (2010) is shown in Figure 2.

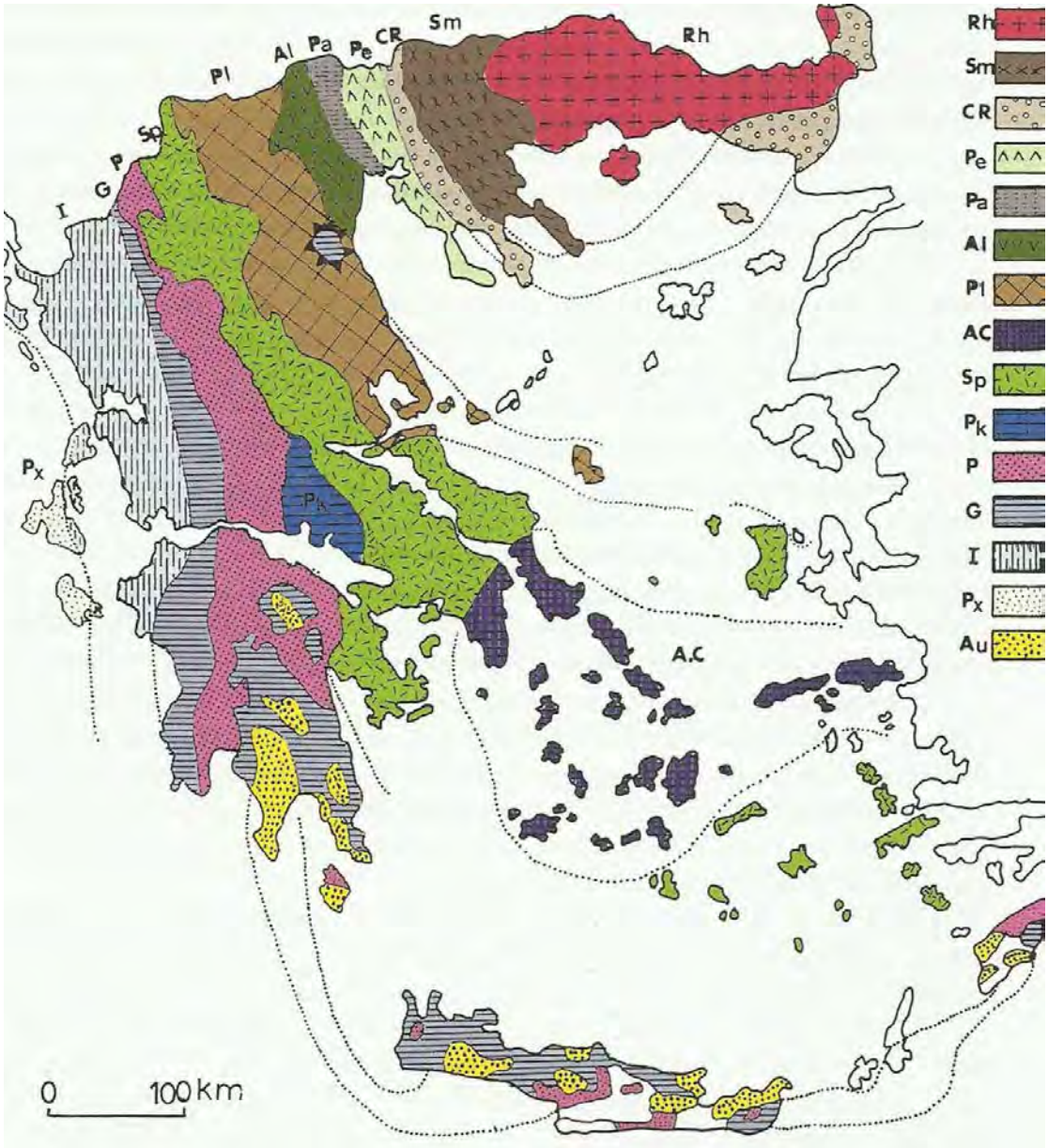

Figure 2: The geotectonic zone separation of Greece. The symbols stand accordingly as Rh: Rhodope massif, Sm: Serbomacedonian massif, CR: Circum Rhodope zone, Ax: Axios zone = (Pe: Peonia subzone, Pa: Paiko subzone, Al: Almopia subzone), Pl: Pelagonian zone, AC: Atticocycladic zone, Sp: Subpelagonian zone, Pk: Parnassos zone, P: Pindos zone, G: Gavrovo zone, I: Ionian zone, Px: Paxoi zone, Au: Plattenkalk (Mountrakis 2010).

The study area in this B.Sc. thesis lies within the Almopia subzone which is part of the greater Axios zone. The subdivision of the latter into Peonia, Paiko and Almopia subzones was made by Mercier (1968) and it's still in use, with minor changes, until this day as shown in Figure 3.

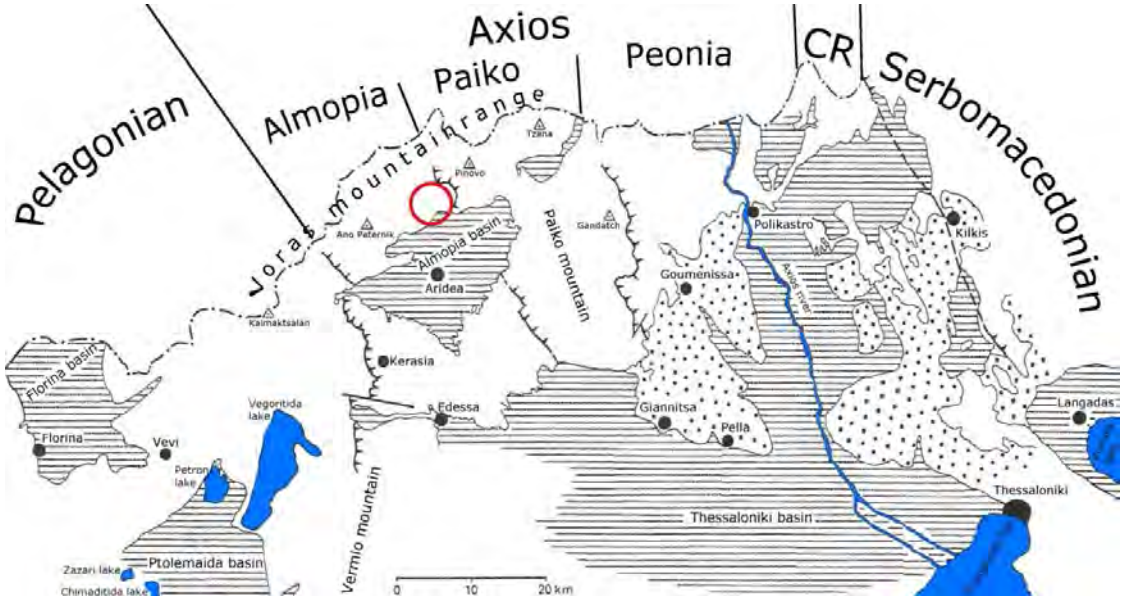

Figure 3: The subdivision of Axios zone to Almopia, Paiko and Peonia subzones. The study area is shown with a red circle (modified after Mercier 1968).

Axios zone, named after the big homonymous river of central Macedonia, is a land strip of 30-70km width and NNW-SSE direction between the Circum Rhodope and the Pelagonian zones. It starts from the borders of FYROM with Greece, continues through the Thermaicos gulf and then disappears beneath the Aegean sea. It is believed that after Thermaicos gulf, the zone probably takes a W-E to SW-NE direction and reemerges in Asia Minor.

The main characteristic of Axios zone is the presence of extensive ophiolite rocks with accompanying deep sea sediments, which lead geoscientists to make the assumption that during the past the area consisted of oceanic lithosphere and was covered by an ocean. The subdivision of Axios zone into Peonia, Paiko and Almopia subzone by Mercier (1968) and other geoscientists was based on the observations that the sediments found in each subzone were formed in different sea levels and thus were representative of various depths in the ancient ocean. More specifically the sediments found in the Paiko subzone were neritic, mostly recrystallized limestones and indicative of a shallow sea. In contrast, the sediments found around the Paiko subzone, namely the sediments of Almopia and Peonia subzones, were originated definitely from greater ocean depths because they consist of clays and/or cherts and other deep sea sediments. So, this sediment differentiation along with the presence of volcanic and volcanosedimentary materials in the Paiko subzone lead geoscientists to consider the latter, in the past, as a volcanic island arc with shallow sea sedimentation surrounded by the deep sea areas of Almopia and Peonia subzones.

The aforementioned theory is believed as the initial interpretation and is still supported by many geoscientists although new evidence tends to tumble it.

New theories have emerged through the years proposing different geological and tectonic models but one of them seems more appropriate considering the new data. This new theory (Kilias et al. 2010, Katrivanos et al. 2013) claims that an ocean did

exist but it was placed not in today's land mass strip called Axios zone but further away to the northeast. The presence of ophiolite rocks with the accompanying deep sea sediments in Axios zone is explained as an obducted allochtonous nappe, placed in its current position during the orogenic movements that gradually formed today's tectonic landscape.

Mercier (1968) further subdivided every subzone in Axios zone into smaller tectonic units, a subdivision that is also in use today with minor changes. The more important tectonic units considering Almopia subzone are shown in Figure 4.

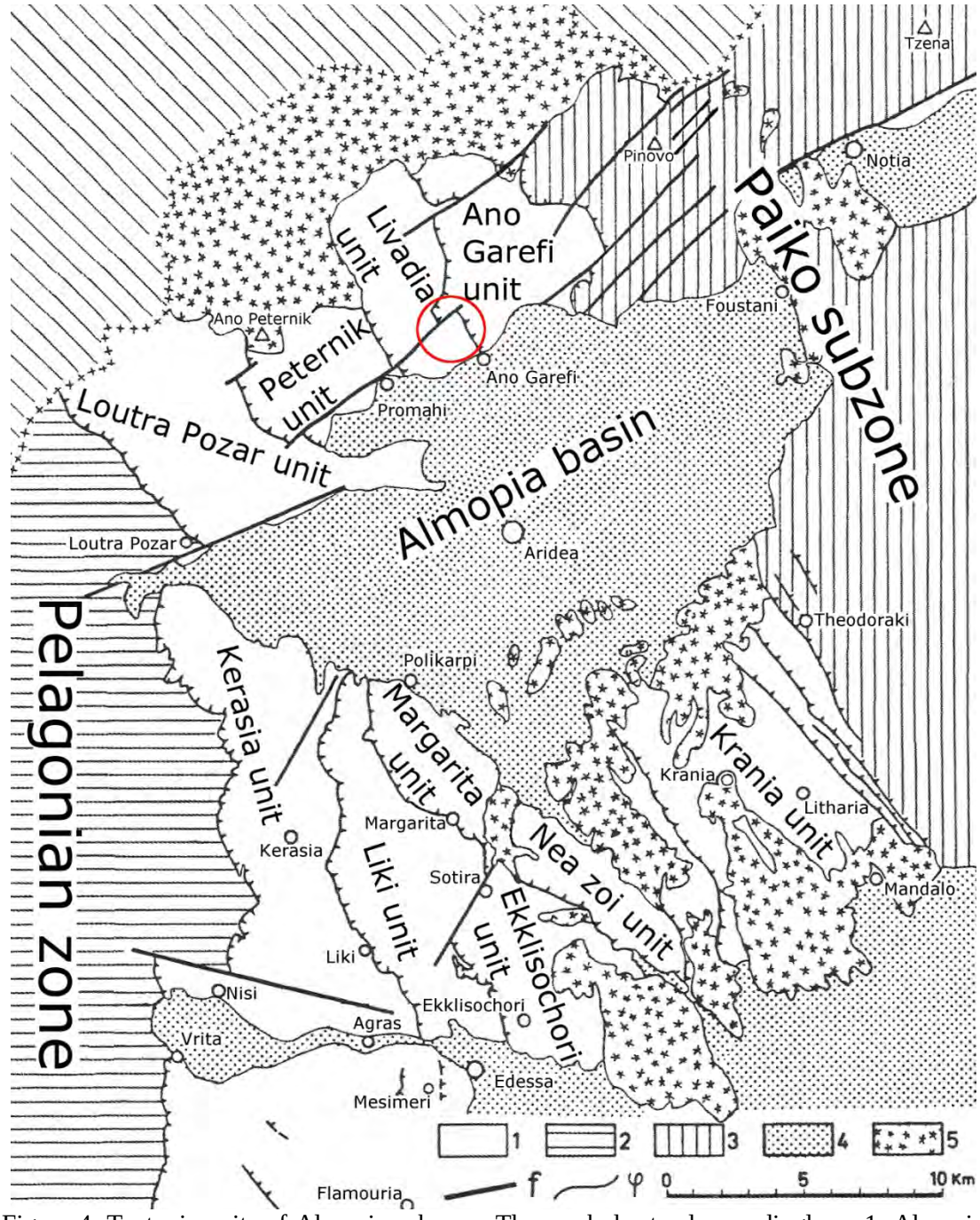

Figure 4: Tectonic units of Almopia subzone. The symbols stand accordingly as 1: Almopia units, 2: Pelagonian zone, 3: Paiko subzone, 4: Quaternary sediments, 5: post alpine volcanics, f: faults, φ: unconformities. The study area is shown with a red circle (modified after Mercier 1968).

The subdivision into smaller tectonic units isn't implying a great change in terms of the geology between them. In contrast, the geology is considered to be the same and only small changes can be found locally. So, the subdivision was made for a different purpose which was to highlight the area's tectonic state. The tectonic of Almopia is characterized by the continuous thrust of one tectonic scale onto another forming the so called Almopian tectonic scales. So, every tectonic scale is actually made up by the same lithologic formations, although some of them may be absent in some specific areas.

In general, the main lithologic formations of the Almopia subzone are shown in Figure 5.

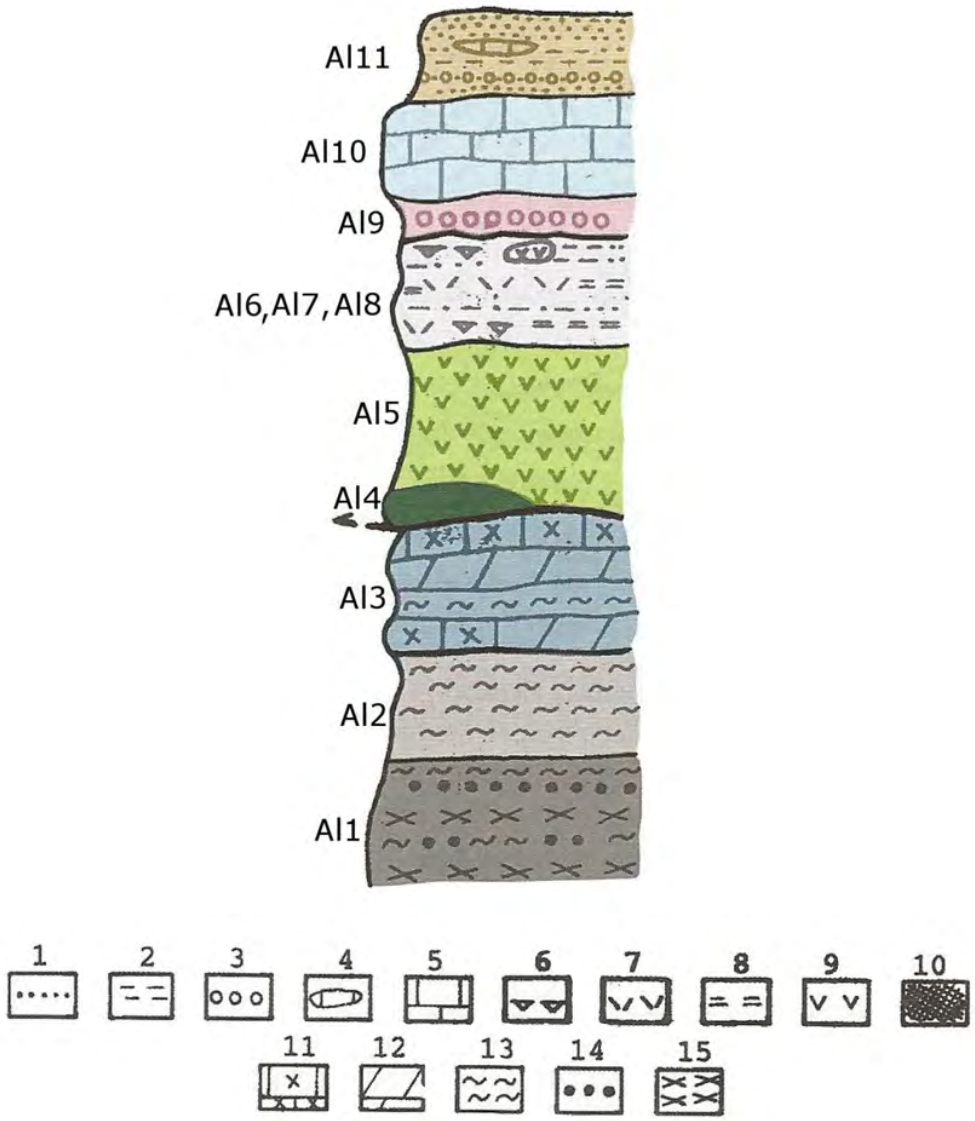

Figure 5: Generalized lithostratigraphic column of Almopia. The symbols stand accordingly as 1: sandstone, 2: clay and slates, 3: conglomerates and other clastic sediments, 4: calcareous lenses, 5: limestones, 6: cherts, 7: volcanic materials, 8: tuffs and volcanoclastics, 9: ophiolites, 10: ophiolitic melanges, 11: marbles and crystalline limestones, 12: dolomites, 13: schists, 14: amphibolites, 15: gneisses (modified after Mountrakis 2010).

Mountrakis (2010) gave the following descriptions regarding each formation.

Al1 consists of strongly metamorphosed rocks such as augen gneisses and amphibolites alternating in the upper parts with quartzites, amphibolitic schists, mica

schists and chloritic schists. The age of this formation is thought to be pre-Alpine (Paleozoic) and probably belongs to the Pelagonian basement. It seems that the obducted ophiolites and oceanic sediments overlie this formation. Al1 can be found in the Peternik unit.

Al2 consists of calcareous schists, chloritic schists, sericitic schists, phyllites, sipolines and marbles of Triassic to maybe Jurassic age. These rocks are also metamorphic and alternate each other many times due to the tectonic nappe pile stacking. Al2 can be mainly found in Loutra Pozar unit and Peternik unit but also in some southern units as well.

Al3 consists of marbles, crystalline limestones, dolomites and intercalations of schists. These rocks can be found in the same places as Al2. It seems that Al3 is the continuation of Al2 and they represent the Triassic-Jurassic sedimentation.

Al4 consists of ophiolitic melanges which are tectonically emplaced onto the previous formations. This is a tectonic formation and was created during the obduction of the ophiolites onto the continental crust. Inside the melanges there can be found big or small marble and other metamorphic blocks set in an ophiolitic mass. The emplacement probably happened during Upper Jurassic. Melanges can be found in various places in the Almopia subzone but the most characteristic appearance of these rocks lies within the Ekklisochori unit.

Al5 is considered as the most important formation of Almopia subzone and consists of ophiolites (serpentinites, basic lavas, dolerites etc). The age of the ophiolites is Jurassic and the tectonic emplacement is thought to be Upper Jurassic.

Al6, Al7 and Al8 are referred as one formation but there are many differences from place to place. They consist of sedimentary (Al6), volcanosedimentary (Al7) and clastic (Al8) materials. They are found on top of the ophiolites but also synfold with them as they are the accompanying deep sea oceanic sediments. The age of this formation is similar to the ophiolites' age. They have been obducted onto the land synchronously with the ophiolites in Upper Jurassic. More specifically they consist of radiolaritic cherts, claystones, slates, sandstones, pelagic limestones and calcareous schists. In some places there can be found neritic limestone banks. The clays and sandstones may form turbiditic flysch-like layers.

Al9 represents the basal conglomerate deposited during the Upper Jurassic retrogression. This first retrogressive formation is better observed in Kerasia and Loutra Pozar units.

Al10 is a typical retrogressive formation of Upper Jurassic (Santonian) consisting of grey to black limestones.

Al11 is a flysch of Upper Jurassic (Maastrichtian) to Paleocene age consisting of sandstones, sand limestones, calcareous schists and conglomerates.

The formations that can be observed, close to the area in which the samples were found, are from Al4 and up (Al1, Al2 and Al3 are not visible). The main formation of course is the ophiolites, consisting of serpentinized harzburgites and dunites which are the host rocks of the rodingites. According to Migiros and Galeos (1990) these rocks can't have a continental origin although their analyses show otherwise. So it is concluded, in their research, that they were probably formed at a basin along a rifted continental margin.

A small part from the geological map of Promahi constructed by Galeos et al. (1979-1983 and 1997) in 1:50000 scale which shows the aforementioned lithologic formations near the study area is shown in Figure 6.

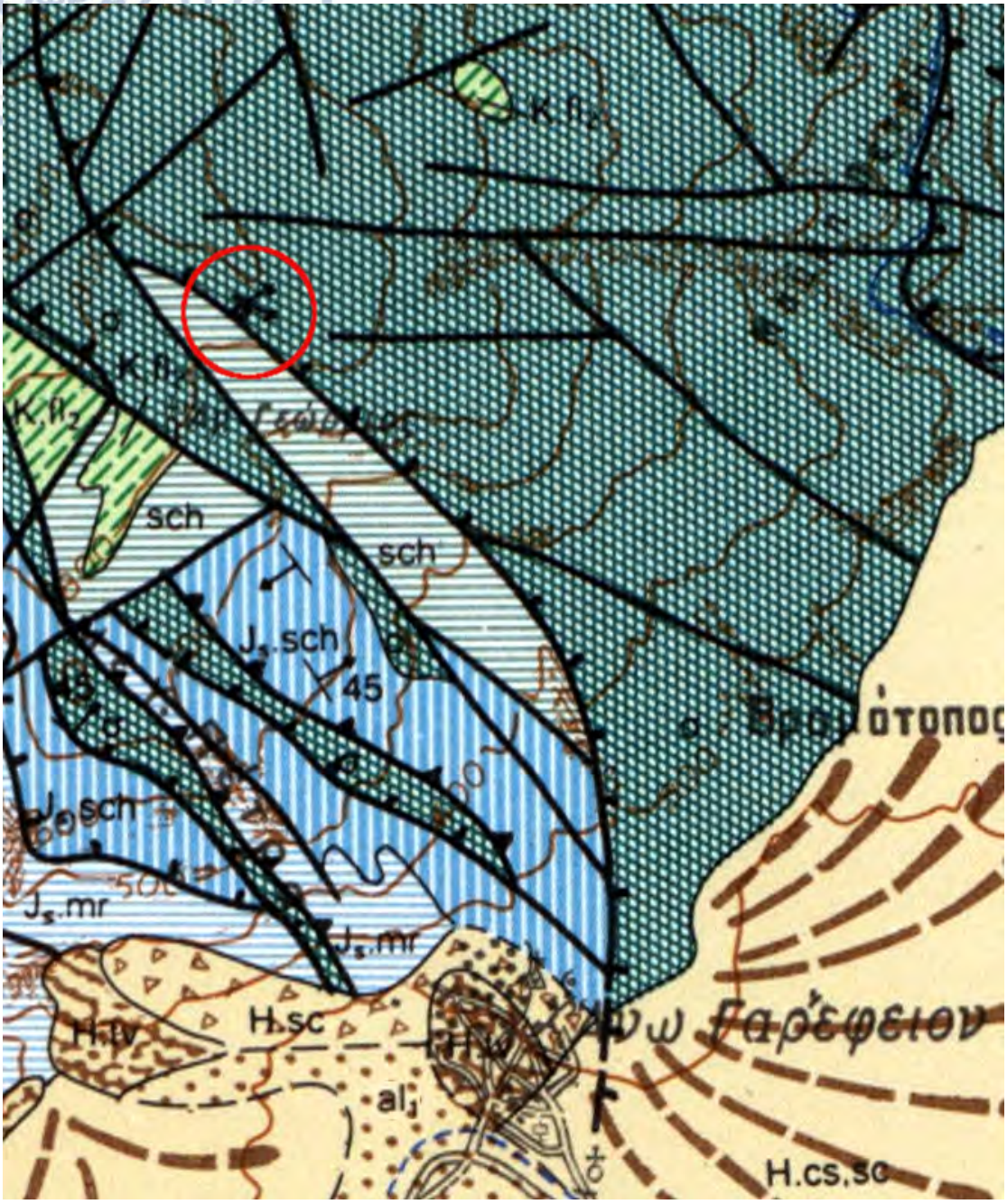

Figure 6: A small part of a geological map focusing on the study area. The samples' area is shown with a red circle (modified after Galeos et al. 1979-1983 and 1997).

The map's legend gives the following specifications for each formation, from bottom to top.

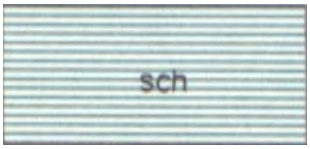

prasinites-greenschists of Upper Jurassic age, constituting the basal tectonic melange. They occur mainly in the western part, underlying the ophiolitic thrust sheets following the same direction. They consist mainly of chlorite-epidote-actinolite schists with feldspars (plagioclase), biotite, muscovite, quartz, calcite, sericite, of initial basic volcanic-pyroclastic to subvolcanic origin. Prasinitic

meta-breccia-conglomerate layers frequently occur, strongly deformed, with volcanic (basic or acid) and carbonate elements. They are bedded and cohesive. The thickness is exceeding 200m locally.

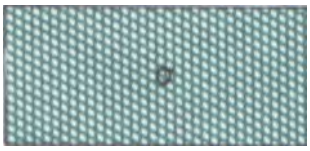

ultrabasic rocks of Upper Jurassic age, which form a tectonic pile of ultrabasic thrust sheets consisting of serpentinized dunites and mostly serpentinized harzburgitic tectonites. Locally, the ultrabasites are traversed by diabase veins, 0.20-1.5m thick, with directions parallel to the main faulting zones, as well as by rodingitized gabbrodioritic veins (Migiros and Galeos 1990). The visible thickness of the tectonic pile of peridotitic thrust sheets reaches 1500m.

Livadia schist system with lenticular marble intercalations of Upper Jurassic age. Schists are black-grey to green, mainly calcitic, shales, quartzitic, muscovitic-sericitic while marbles (sometimes microcrystalline limestones) are usually grey when alternating in thin layers and white-whitegrey when they are thick-bedded. They are schistose-lamellar, often dolomitic. Total thickness is estimated at 500m as the formation is strongly folded and foliated.

transgressive Upper Cretaceous flyschoid series of Promahi-Garefi occurring north of Ano Garefi village. The transgression starts with basal conglomerate and passes into alternations of grey-black calcitic, sericitic phyllites (siltstones) and sandstones, with thin black limestone intercalations. Upwards the limestone participation increases in number and thickness reaching 30 to 50m northwards of Promahi village. They are bedded to massive, always with schistose structure. Sparse occurrences of the formations' base, consisting of ophiolitic breccio-conglomerates and sandstones, occur in cavities of the ophiolites' surface. North of Ano Garefi village the transgressive Upper Cretaceous formation lies on the prasinites. They are small occurrences of grey-black, pseudocondular limestones, alternating with black calcitic siltstones to phyllites. Small rudists, gastropods, lamellibranches, algae (?), were found in the limestones. The maximum visible thickness is 250m approximately.

travertine of Quaternary age.

old and recent Quaternary talus cones and scree.

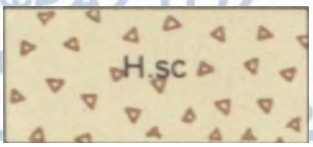

Quaternary scree.

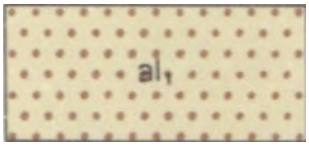

recent fluviolacustrine silt and gravel deposits.

A cross-section was included in the map which helps the reader to better understand the area's tectonic evolution. The following cross-section (Figure 7) is a small part of the primary but gives a clear image of the area's geology although that it cross-cuts an area which lies a little bit northern of the study area.

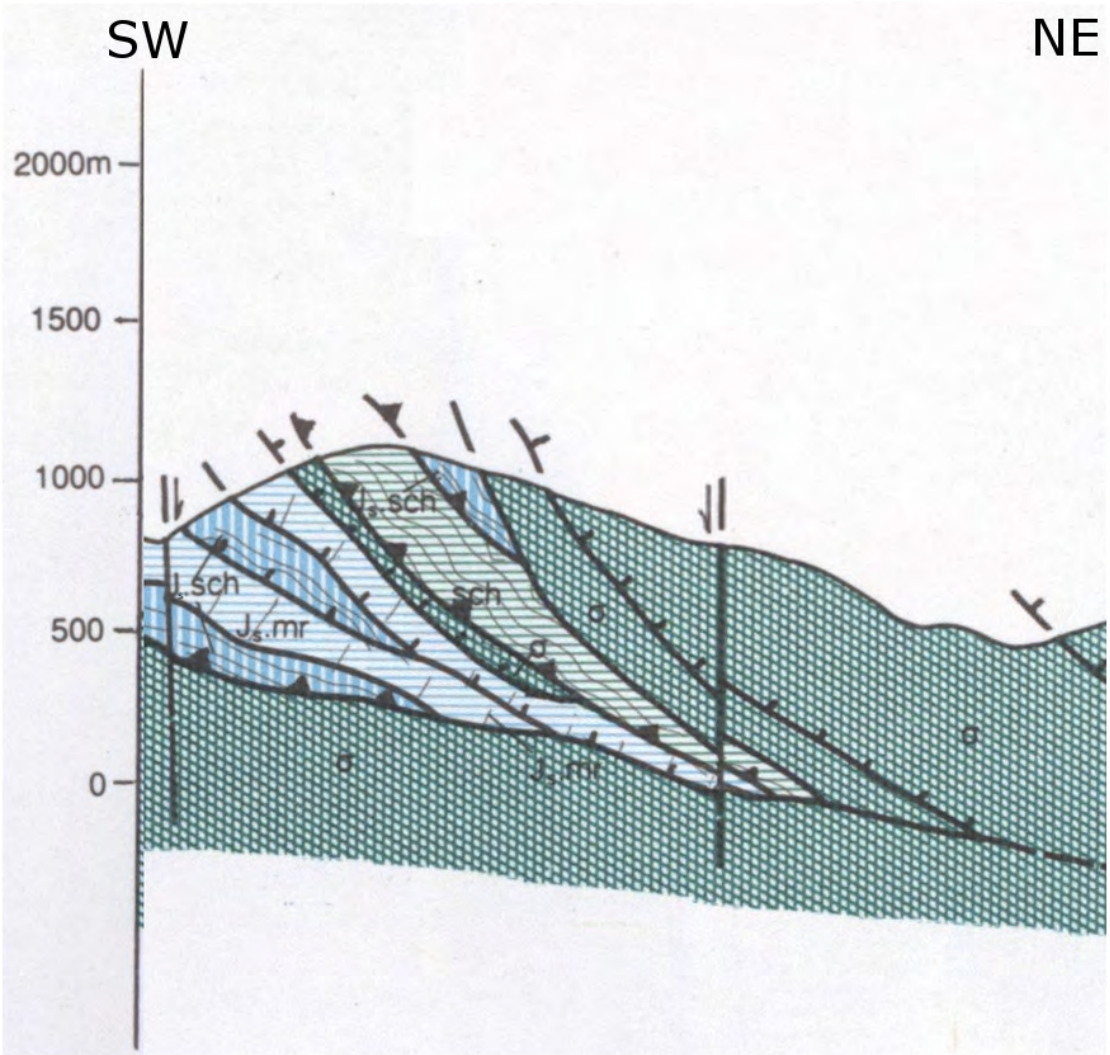

Figure 7: Cross section near the study area showing the main tectonic events (modified after Galeos et al. 1979-1983 and 1997).

5. The Ano Garefi rodingites

5.1. Previous research

With the exception of Galeos et al. (1979-1983 and 1997) and Migiros and Galeos (1990), simply mentioning the existence of rodingites within the ophiolites, no other scientific paper about these rocks was found by the writer.

5.2. Rodingites in the field

The Ano Garefi rodingites occur as pods, veins and blocks enclosed in serpentinites and usually adjacent to small or large tectonically included carbonate bodies. As already mentioned in the introduction, these copper bearing rodingites can be regarded as an exception to the rule that in most cases rodingites tend to be barren rocks without the presence of ore mineralization. The Ano Garefi rodingites are distinct rock outcrops due to their light color and conspicuous contrast with the dark-colored serpentinite host rocks. The biggest rodingite outcrops occur as blocks, exceeding 2m in thickness and are found as reaction zones between serpentinite and carbonate bodies (Figure 8).

Figure 8: A field image of the Ano Garefi rodingites. The main picture, which is the enlargement of the red rectangle in the reference image, shows an exploration mining gallery created probably around 1912. The red dotted line represents the boundary between the rodingite block with the carbonate body at the bottom left corner and the surrounding serpentinites at the top right corner. The rodingite block exceeds 2m in terms of thickness.

Macroscopically, these rodingites have a pale green-brown color while their minerals are medium- to coarse-grained. The ore minerals, mainly consisting of chalcopyrite, due to their color and hue are very characteristic and they occur either as small or even locally as large segregations or thin veinlets. Malachite, which forms after disintegrated chalcopyrite, is usually a good index for spotting these rocks. Images of rodingite hand specimens from Ano Garefi are shown in Figures 9 and 10.

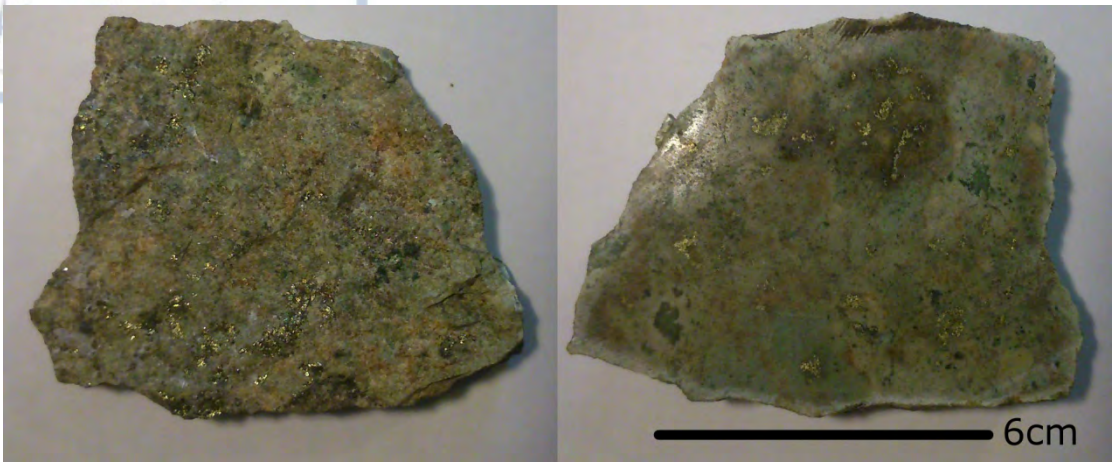

Figure 9: A sectioned rodingite hand specimen from Ano Garefi. The images are taken before (left) and after (right) the sectioning by a cutting wheel.

Figure 10: A rodingite hand specimen from Ano Garefi.

5.3. Petrography

Mineral identification and textural relationships were established using optical microscopes, and conducting electron probe microanalyses with a SEM. Therefore, it was realized that the mineral constituents were spatially found in highly variable proportions having a fine- to coarse-grained texture.

The identified mineral assemblages consist of calcite + garnet + epidote + clinopyroxene + chlorite ± chromite + chalcopyrite ± pentlandite ± sphalerite. The aforementioned paragenesis was initially recognized by using transmitted and reflected light microscopes and confirmed after that by conducting electron probe microanalyses. Under the microscope, the mineral constituents of rodingites resemble that of skarns and can easily be mistaken with these rocks. After all, both rodingites and skarns are contact metamorphic rocks, enriched in terms of Ca, so it is unexpected for these rocks to look alike.

Calcite occurs as clasts enclosed inside the rodingitized mass, which in some cases are quite large. Besides, veins or even extended aggregates of calcite crystals

including silicate minerals are found. It has also been observed, in some of the thin sections, an extended contact between the calcite and the silicate minerals, which is either the boundary of the two different lithotypes, namely the rodingite block and the carbonate body, or probably represents the replacement front of the rodingitization. Transmitted light images of calcite are shown in Figure 11.

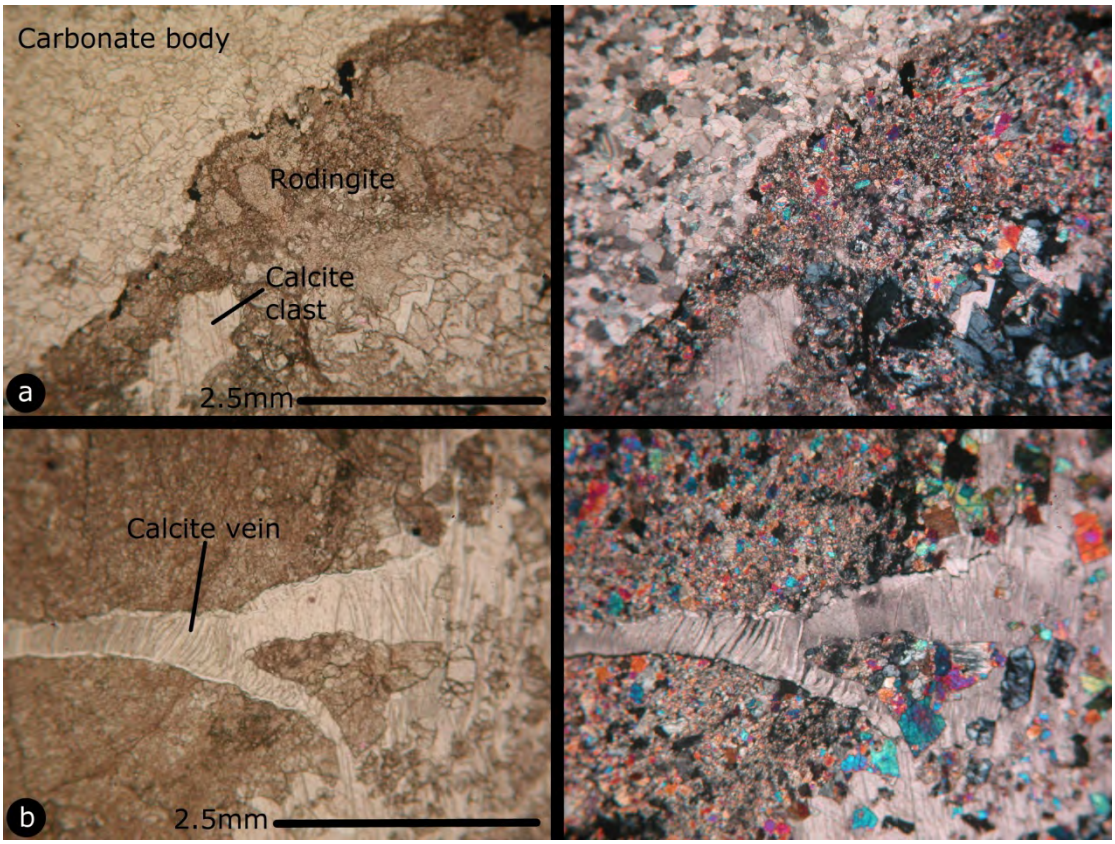

Figure 11: Transmitted light images of calcite. (a) the rodingite-carbonate body boundary and a calcite clast near the contact. (b) a ramified calcite vein. The right images are taken with crossed polars.

Calcite could be a residual primary mineral or a secondary one. The clasts that were found enclosed inside the rodingite must come from the carbonate body and thus be residual primary calcite. The fact that most calcite clasts are found near the contact between the rodingites and the carbonate bodies (Figure 11a) strongly suggests that these pieces were actually detached from the latter by the hydrothermal fluids and entrapped inside the rodingites after their formation. On the other hand, the calcite veins (Figure 11b) must be constituted by secondary calcite due to the fact that inside the veins are enclosed minerals being typical of rodingites such as garnets, epidotes and clinopyroxenes.

The silicate minerals garnet, epidote, clinopyroxene and chlorite constitute volumetrically the most important silicate minerals of the studied rodingites from Ano Garefi.

Garnet is abundant and occurs in well shaped euhedral crystals. It is worth noting that most of the garnet crystals display marked birefringence and are anisotropic when examined with crossed polars in the transmitted light microscope, despite the fact that garnets are by rule isotropic. As a result, they show low first order interference colors. A sector zoning from core to rim can also be observed in some garnets. In some cases, the rim of the crystal seems either to be optically differentiated from the core or to be

occupied by a different mineral causing the optical zonation. Electron probe microanalyses showed that the narrow-width rim is actually occupied by another mineral, which is epidote.

Apart from the garnet's rim, epidote also forms separate crystals, some of which are quite impressive due to their euhedral and prismatic shape.

Clinopyroxene is also abundant. The crystals that were found in the thin and thin-polished sections can be characterized mainly as subhedral but euhedral crystals can be found as well.

Chlorite has a pale green color and forms small flakes that can be found interstitially to the other minerals. Transmitted light images of silicate minerals are shown in figure 12 while backscatter electron images are shown in Figure 13.

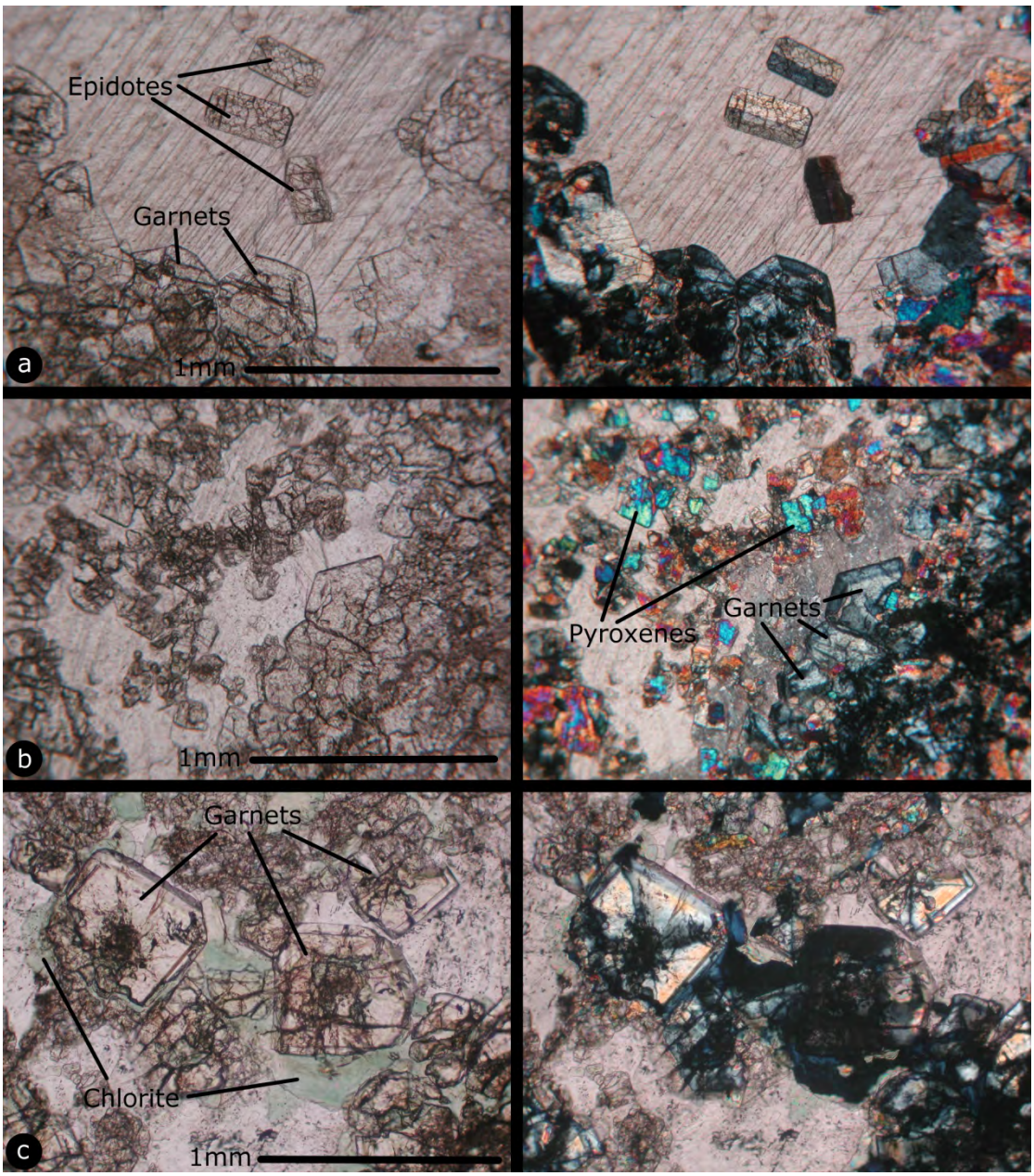

Figure 12: Transmitted light images of silicate minerals. (a) prismatic epidote crystals and garnets. (b) garnets and pyroxenes. (c) chlorite flakes occupying the interstitial space between the other crystals. The right pictures are taken with crossed polars.

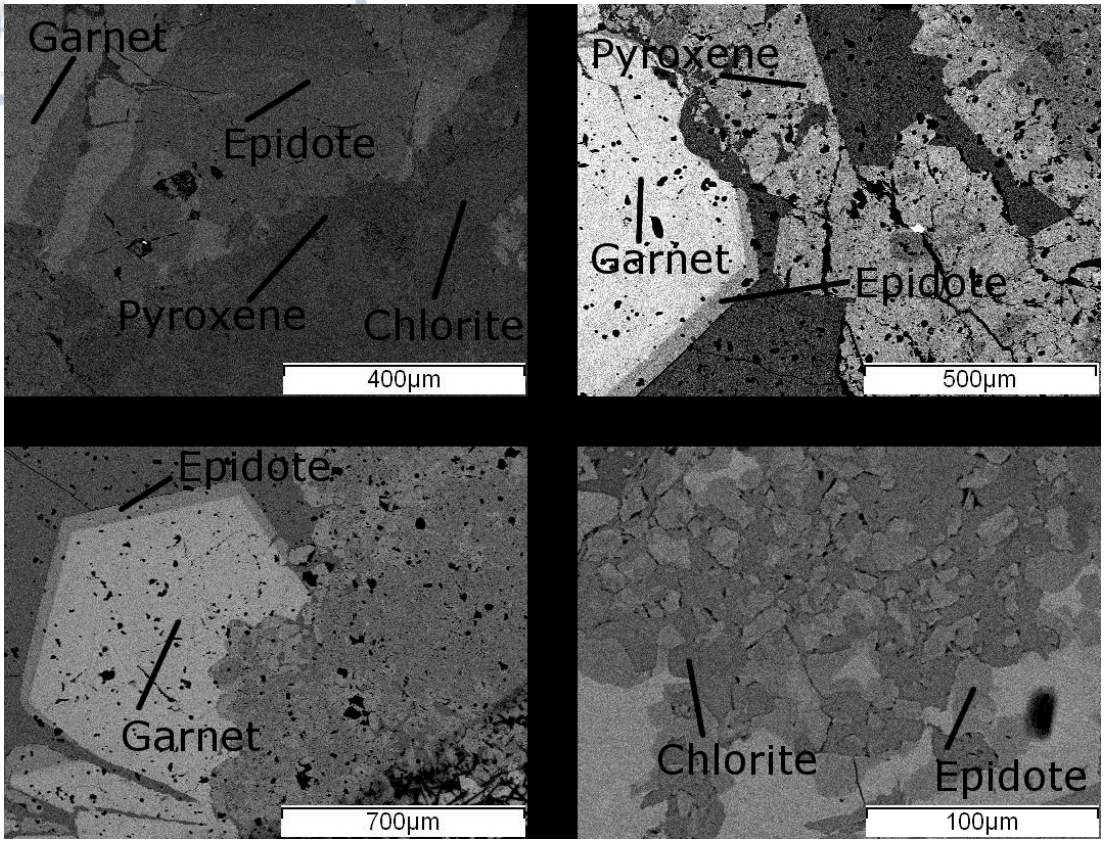

Figure 13: Backscatter electron images of rodingites showing the silicate minerals as different shades of grey.

Chromite is the only primary mineral preserved in the rodingite samples being a relict mineral from the serpentinite rock entrapped inside the rodingites during the formation of the latter.

When observed in transmitted light (Figure 14), the chromite grains show a brown-red color in the core, while their marginal areas are opaque. The opaque edges are the result of the alteration of the chromite crystals into ferritchromite, a term used by Spangenberg (1943) and cited by many others (e.g. Beeson and Jackson 1969, Ulmer 1974, Michailidis 1990, Merlini et al. 2009, Saumur and Hattori 2013).

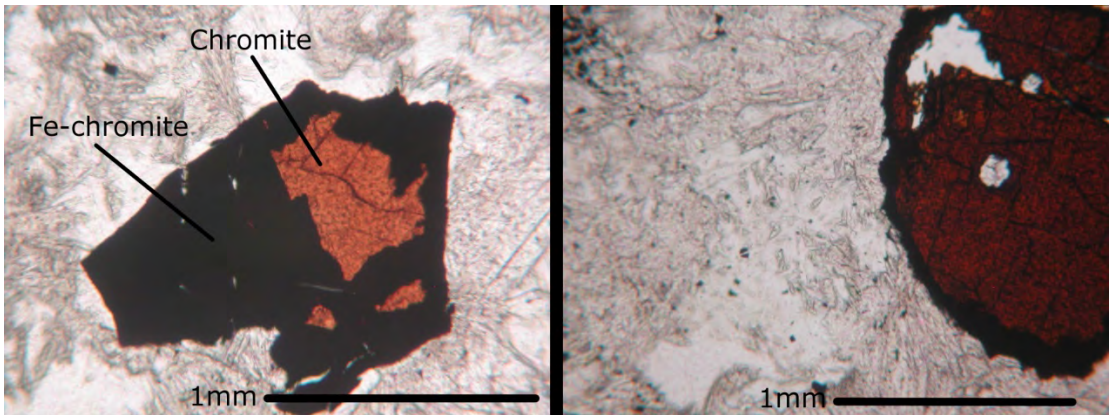

Figure 14: Transmitted light images of chromite crystals. The unaltered chromite crystals are shown with a brown-red color while the marginal areas of the grains are opaque, indicating an alteration of the primary mineral into ferritchromite.

When observed in reflected light, chromite occurs as small and fractured clasts, showing evidence of tectonic deformation (Figure 15).

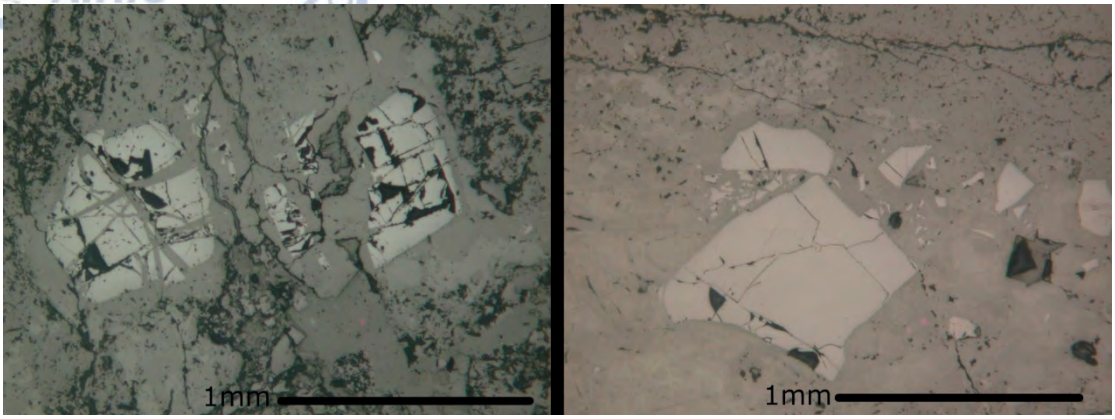

Figure 15: Reflected light images of fractured chromite clasts.

The most important findings regarding this B.Sc. thesis, differentiating the specific rodingites from the common rodingites, are the ore minerals consisting mainly of chalcopyrite and in very small percentages (less than 10% of the mass of the ore minerals) by pentlandite and sphalerite as well as by surficially formed malachite and goethite. These minerals can be found as local segregations connected together by an extended network of small veinlets. The segregations fill the interstices between the other minerals such as the silicates or calcite. The size of these segregations may vary a lot ranging from very small to very large, sometimes exceeding locally 1.5cm in length. The sulfide mineral content approximately accounts for about 5% by volume of the rodingite body.

Chalcopyrite accounts as the main mineral regarding the sulfides. Under the reflected light microscope, chalcopyrite has a typical vivid yellow color and forms an extended network of small veinlets. These veinlets are found interstitially to the gangue minerals and in some cases incorporating small or even big aggregates of them, indicating that chalcopyrite formed at a later stage after the formation of the other minerals. In backscatter electron images, chalcopyrite is easily spotted from the gangue minerals due to its high contrast, resulting in depicting this mineral with brighter shades of grey.

Pentlandite, under the reflected light microscope has a typical sparkling yellow-white color which is similar to that of pyrite and can easily be mistaken with it. Pentlandite occurs in close contact with the chalcopyrite. It forms small and well shaped crystals, sometimes partly replaced by chalcopyrite or by silicate minerals. It's origin from the serpentinite protolith cannot be excluded. It is difficult to distinguish pentlandite from chalcopyrite in the backscatter electron images because both of these minerals are depicted with bright shades of grey.

Sphalerite has the typical grey color under the reflected light microscope and also occurs in close contact with the chalcopyrite forming irregular aggregates. Along with chalcopyrite they fill the interstices between the other minerals. Sphalerite must have formed at the same time with chalcopyrite. In backscatter electron images, sphalerite has been always found in contact with chalcopyrite. In terms of the grey scale, sphalerite is a little brighter than chalcopyrite.

Reflected light images of the ore minerals are shown in figure 16 while backscatter electron images are shown in Figure 17.

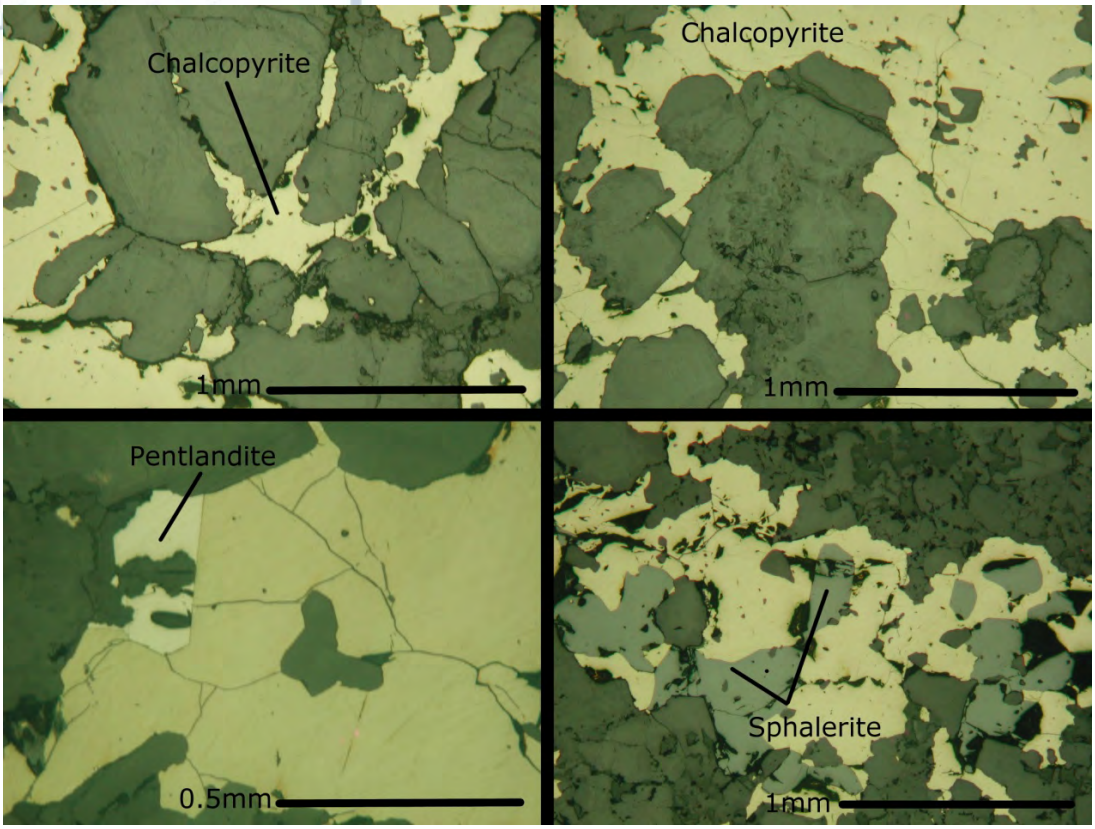

Figure 16: Reflected light images of the ore minerals.

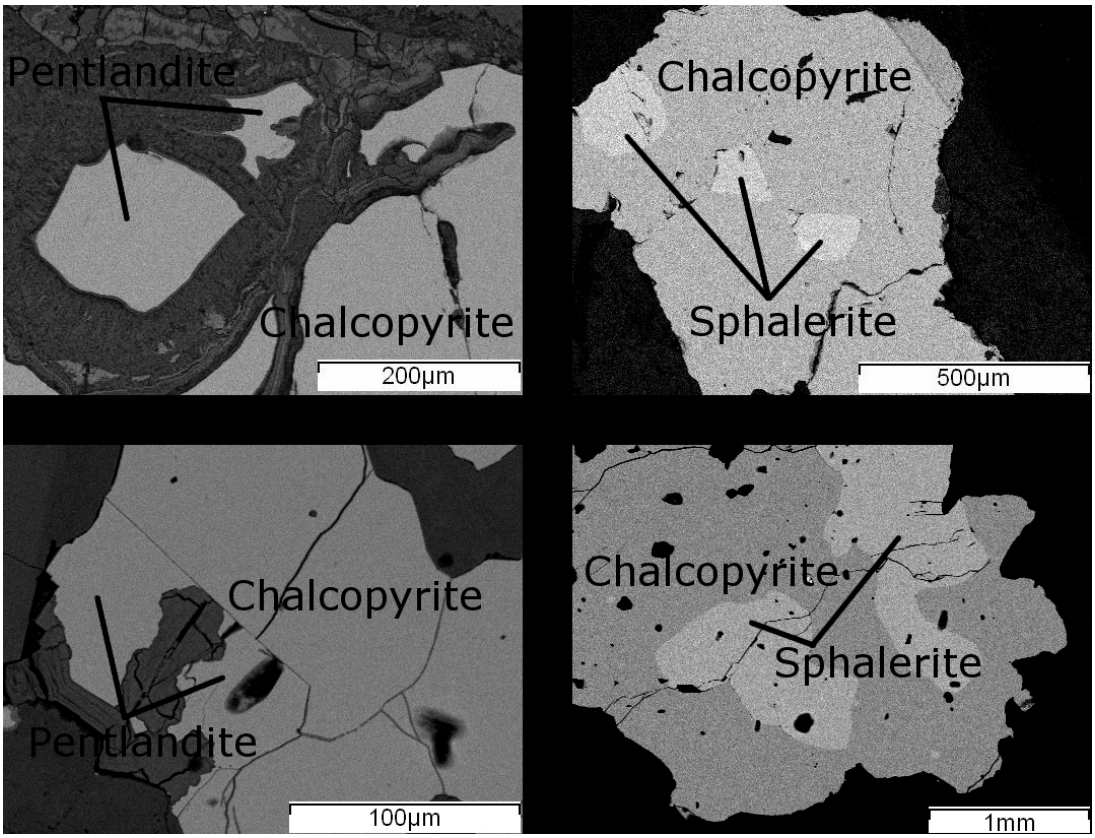

Figure 17: Backscattered electron images of the ore minerals. Distinguishing pentlandite from chalcopyrite in these images is not easy.

6. Mineral chemistry

6.1. Analytical methods

Some thin-polished sections of the rodingites were prepared for SEM-EDS microanalyses.

SEM-EDS investigation was carried out at the Aristotle University of Thessaloniki using a JSM-840A Scanning Electron Microscope (SEM) equipped with a LINK system Energy Dispersive Spectrometer (EDS) INCA 300. Operating conditions were: accelerating voltage 20kV, beam current 0.4mA, beam diameter 1μm and counting time 80 seconds.

Corrections were made using the ZAF-4/FLS software provided by LINK. Recalculation of electron probe microanalyses for the estimation of ferrous and ferric iron, water content, along with the molecular proportions of the end-members in the different minerals was made using the spreadsheets found in the website of the Science Education Research Centre (SERC) of Carleton College (http://serc.carleton.edu/research_education/equilibria/mineralformulaerecalculation.html). These programs are open source and were made, unless otherwise mentioned, by John Brady of Smith College and Dexter Perkins of University of North Dakota.

6.2 .Silicate minerals

6.2.1. Garnet

Garnets form a large group of minerals and their structure can be described by the chemical formula: $X_3Y_2Z_3O_{12}$, where the X site is filled by divalent cations such as Mg, Fe, Mn and Ca, the Y site is filled by trivalent cations such as Al, Fe, Ti and Cr while the Z site is filled by Si. The combination between these chemical elements can theoretically lead to the formation of up to 16 different garnet species or end-members. However, this group can roughly be described by two isomorphous series, namely the pyralspites and the ugrandites, each containing three end-members that are most common found in nature (Table 1).

Table 1: The subdivision of pyralspites and ugrandites into garnet end-members.

	Garnet end-members	**Chemical formula**
Pyralspites	Pyrope	$Mg_3Al_2Si_3O_{12}$
	Almandine	$Fe_3Al_2Si_3O_{12}$
	Spessartine	$Mn_3Al_2Si_3O_{12}$
Ugrandites	Uvarovite	$Ca_3Cr_2Si_3O_{12}$
	Grossular	$Ca_3Al_2Si_3O_{12}$
	Andradite	$Ca_3Fe_2Si_3O_{12}$

A naturally occurring garnet with a pure end-member composition is considered to be rather rare. A solid solution between different end-members is more common and the name is thus ascribed to the garnet by the dominant ‘molecular’ type. Variations in the chemical composition don’t seem to occur between the two series but mainly

through pyralspites or ugrandites separately. Although, some other chemical elements can be found in garnets, the aforementioned are the most common (Deer et al. 1992).

Selected microanalyses of garnets from Ano Garefi are presented in Table 2 and a ternary plot in terms of three garnet end-members, using the dominant andradite and grossular and combining together the end-members of pyrope and spessartine, is shown in Figure 18.

Table 2: Selected microanalyses of garnets from Ano Garefi.

bdl: below detection limit	1	2	3	4	5	6	7
Oxide weight %							
SiO_2	38,51	38,81	35,91	37,33	37,92	36,59	36,64
TiO_2	0,32	2,27	0,90	0,66	0,46	bdl	bdl
Al_2O_3	10,10	8,53	5,10	7,53	6,41	8,60	6,52
Cr_2O_3	bdl	bdl	bdl	bdl	bdl	bdl	bdl
Fe_2O_3	12,85	13,27	19,15	16,15	17,32	16,29	17,91
FeO	2,77	bdl	4,50	2,68	2,97	2,04	4,34
MnO	bdl	1,48	0,56	0,19	0,49	0,79	0,74
MgO	bdl	0,36	bdl	0,01	0,42	bdl	0,04
CaO	34,94	35,56	33,58	35,21	34,37	35,98	33,71
Total	99,50	100,28	99,71	99,77	100,36	100,28	99,90
Ion distribution based on 12 (O)							
Si	3,088	3,084	2,992	3,040	3,079	2,973	3,023
Al	-	-	0,008	-	-	0,027	-
Al	0,987	0,827	0,519	0,754	0,642	0,832	0,665
Ti	0,019	0,136	0,056	0,041	0,028	-	-
Cr	-	-	-	-	-	-	-
Fe^{3+}	0,776	0,794	1,201	0,990	1,059	0,996	1,112
Fe^{2+}	0,186	-	0,314	0,182	0,202	0,138	0,300
Mn	-	0,100	0,040	0,013	0,034	0,054	0,051
Mg	-	0,042	-	0,001	0,051	-	0,005
Ca	3,003	3,028	2,997	3,073	2,991	3,132	2,980
Total	8,059	8,011	8,127	8,094	8,085	8,153	8,135
End-members (mol %)							
Almandine	0,00	0,00	0,00	0,00	0,00	0,00	0,00
Andradite	44,83	49,82	70,58	57,79	63,31	54,74	63,69
Grossular	55,17	44,23	27,86	41,66	33,32	43,28	34,16
Pyrope	0,00	1,77	0,00	0,05	2,03	0,00	0,18
Spessartine	0,00	4,18	1,56	0,50	1,34	1,98	1,96
Uvarovite	0,00	0,00	0,00	0,00	0,00	0,00	0,00

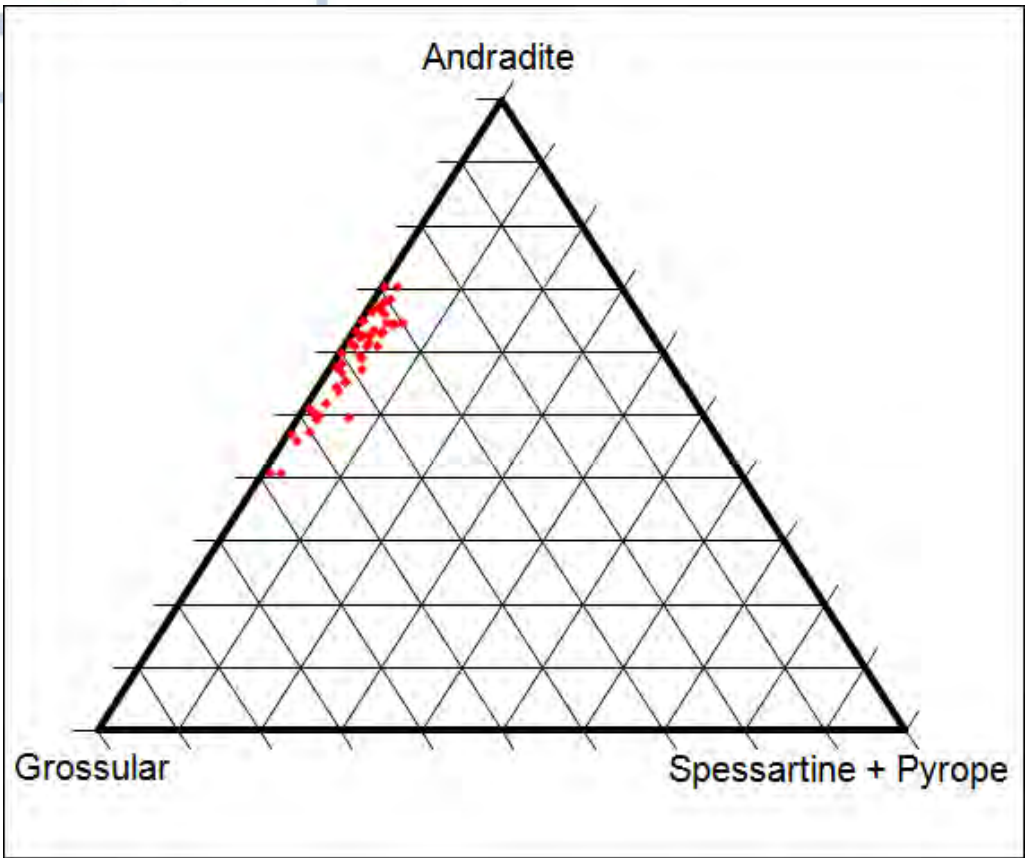

Figure 18: Garnet end-member ternary plot.

In the mineral description, it was mentioned that the Ano Garefi garnets are surrounded by a thin epidotized peripheral zone. A gradual chemical differentiation from core to rim was also observed within the garnet crystal and a typical example of this observation is shown in Figure 19 accompanied by the electron probe microanalyses of Table 3.

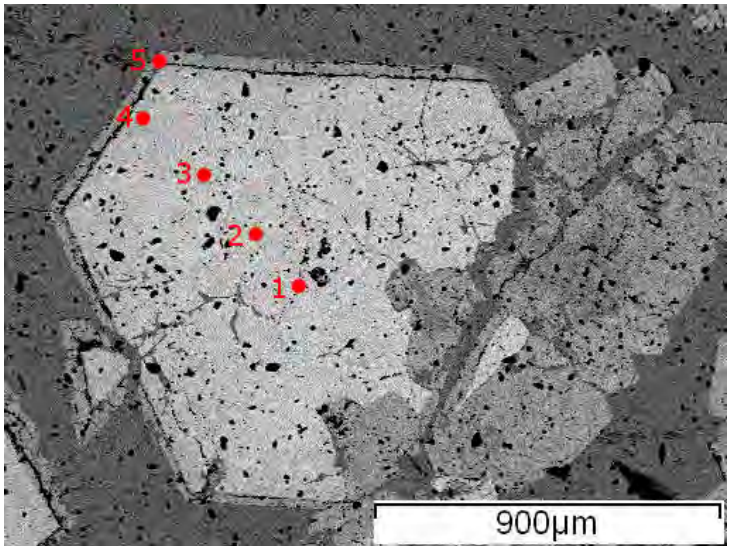

Figure 19: Back scattered electron image of a garnet crystal. This image shows the exact spots of the electron probe microanalyses, directed in a linear array in order to illustrate the chemical differentiation of the garnet from core to rim.

Table 3: The microanalyses for each spot as seen in Figure 19.

bdl: below detection limit	Core → Rim				
Spot	1	2	3	4	5
Mineral	Garnet	Garnet	Garnet	Garnet	Epidote
SiO_2	37,35	37,25	36,84	39,56	39,13
TiO_2	0,02	0,01	0,57	0,04	0,25
Al_2O_3	5,80	5,50	7,19	9,14	17,18
Cr_2O_3	bdl	bdl	bdl	bdl	bdl
Fe_2O_3	17,97	18,87	16,81	13,01	bdl
FeO	6,19	2,33	4,42	3,61	5,88
MnO	0,64	0,38	0,84	0,63	1,89
MgO	0,09	0,12	bdl	0,09	0,09
CaO	31,89	35,63	33,44	33,19	34,23
Total	99,95	100,10	100,10	99,28	98,65
End-members (mol %)					
Almandine	0,00	0,00	0,00	0,00	-
Andradite	66,42	68,65	59,89	47,61	-
Grossular	31,37	29,76	37,86	50,25	-
Pyrope	0,44	0,56	0,00	0,43	-
Spessartine	1,78	1,03	2,25	1,72	-
Uvarovite	0,00	0,00	0,00	0,00	-

According to the electron probe microanalyses presented in Table 2 and the ternary plot of figure 18 it is obvious that the garnets in study belong to the ugrandite series. The dominant garnet end-member is andradite and thus this is the ascribed name to the garnet crystals. Despite that, the garnet's average chemical composition varies somewhere between that of the andradite's and the grossular's. Before the analyses were conducted, it was expected for the garnets to have a composition like this due to the fact that the andradite and the grossular are the varieties of garnets forming together a continuous solid-solution series and are especially characteristic of impure calcareous rocks which have been thermally metamorphosed or of rocks which have undergone calcium metasomatism, such as the rodingites. A chemical differentiation within the crystal is also clear as shown in Figure 19 combined with the data from Table 3. From core to rim, it can be observed an increase in the Al content while the total Fe content is decreasing.

Finally, it must be noted and mentioned that according to various papers and researches about the minerals found in rodingites it is possible that the garnets studied in this thesis are actually hydrogarnets which have the same structure as garnets with the exception of the replacement of one Si^{4+} by $4H^{+}$.

6.2.2. Epidote

The term epidote is not characterizing exclusively one specific mineral but it must rather be perceived as a general concept describing a large and complex group of minerals. The composition for these minerals can be described by the chemical

formula: $X_2Y_3Z_3O_{12}(OH)$ where the X site is filled by Ca, Mg, Mn, Na and K, the Y site with Al, Fe^{3+}, Ti, Cr^{3+} and the Z site is filled by Si and Al^{3+} (Cristofides and Soldatos 2013). Armbruster et al. (2006) in their paper make an effort to highlight the complexity of this vast group of minerals and the difficulty to ascribe specific names to each mineral according to their composition and structure.

However, this group can in general be described by the clinozoisite-epidote series with chemical compositions between $Ca_2Al_3Si_3O_{12}(OH)$ and $Ca_2Fe^{3+}Al_2Si_3O_{12}(OH)$ respectively while the chemical composition of allanite, a mineral that very often contains rare earth elements, is expressed by $REE_2(Fe^{2+},Fe^{3+},Al)_3Si_3O_{12}(OH)$. Zoisite is a polymorph that has the same chemical composition as clinozoisite with the difference that its crystals are of orthorhombic symmetry instead of monoclinic and is thus not considered as a member of the epidote group. In other words, the varieties within this group are the result of substitutions between Al and Fe^{3+} and between $Ca^{2+}Fe^{3+}$ and $REE^{3+}Fe^{2+}$ (Deer et al. 1992).

Selected microanalyses of epidotes from Ano Garefi are presented in Table 4.

Table 4: Selected microanalyses of epidotes from Ano Garefi.

bdl: below detection limit	1	2	3	4	5	6	7
Oxide weight %							
SiO_2	39,78	39,91	38,81	39,13	39,92	38,75	39,42
TiO_2	0,01	bdl	bdl	0,25	0,05	bdl	0,11
Al_2O_3	15,58	17,78	17,65	17,18	16,99	18,82	18,62
FeO	8,42	4,51	5,10	5,88	5,25	5,62	6,32
MnO	bdl	1,91	1,25	1,89	0,84	2,23	1,46
MgO	0,36	bdl	0,18	0,09	0,23	bdl	bdl
CaO	35,10	35,35	36,05	34,23	36,32	34,13	33,82
Na_2O	bdl	0,16	bdl	0,43	bdl	0,21	bdl
K_2O	0,22	0,26	0,20	0,14	0,15	0,08	0,12
Total	99,47	99,88	99,25	99,22	99,75	99,84	99,87
Ion distribution based on 25 (O)							
Si	6,524	6,444	6,334	6,400	6,464	6,283	6,368
Al	-	-	-	-	-	-	-
Al	3,012	3,382	3,395	3,312	3,241	3,597	3,546
Ti	0,001	-	-	0,031	0,006	-	0,013
Fe^{2+}	1,155	0,610	0,696	0,804	0,712	0,762	0,853
Mn	-	0,261	0,173	0,262	0,116	0,306	0,200
Mg	0,087	-	0,045	0,022	0,055	-	-
Ca	6,167	6,115	6,304	5,999	6,300	5,930	5,853
Na	-	0,050	-	0,137	-	0,067	-
K	0,047	0,054	0,043	0,029	0,031	0,017	0,024
Total	16,993	16,916	16,989	16,996	16,925	16,961	16,858

6.2.3. Clinopyroxene

Selected microanalyses of clinopyroxenes from Ano Garefi are presented in table 5 and a ternary plot for their nomenclature after Morimoto et al. (1988) is shown in Figure 20.

Table 5: Selected microanalyses of clinopyroxenes from Ano Garefi.

bdl: below detection limit	1	2	3	4	5	6	7
Oxide weight %							
SiO_2	55,38	51,83	55,56	52,76	53,61	53,38	55,50
TiO_2	0,26	0,31	bdl	0,32	bdl	0,17	0,17
Al_2O_3	0,54	0,74	1,04	0,38	0,24	bdl	0,63
Cr_2O_3	0,11	0,32	0,09	0,44	0,36	0,07	bdl
FeO_{tot}	6,48	6,29	4,84	12,45	13,98	12,83	8,64
MnO	0,17	0,46	0,58	1,23	1,48	2,07	0,52
MgO	11,40	12,13	11,77	8,11	8,03	7,83	11,54
CaO	24,77	27,41	25,73	24,00	22,18	23,54	22,94
Na_2O	0,71	0,41	0,49	0,21	0,03	0,24	0,13
K_2O	0,18	0,09	0,06	0,09	0,24	bdl	0,15
Total	100,00	100,28	99,71	99,77	100,36	100,28	99,94
Ion distribution based on 6 (O)							
Si	2,049	1,934	2,042	2,020	2,050	2,044	2,055
Al	-	0,033	-	-	-	-	-
Fe^{3+}	-	0,033	-	-	-	-	-
Al	0,073	-	0,087	0,037	0,060	0,044	0,083
Ti	0,007	0,009	-	0,009	-	0,005	0,005
Cr	0,003	0,009	0,003	0,013	0,011	0,002	-
Fe^{3+}	-	0,073	-	-	-	-	-
Fe^{2+}	0,201	0,090	0,149	0,399	0,447	0,411	0,268
Mn	0,005	0,015	0,018	0,040	0,048	0,067	0,016
Mg	0,629	0,675	0,645	0,463	0,458	0,447	0,637
Ca	0,982	1,096	1,013	0,984	0,909	0,966	0,910
Na	0,051	0,030	0,035	0,016	0,002	0,018	0,009
K	0,008	0,004	0,003	0,004	0,012	-	0,007
Total	4,009	4,000	3,995	3,986	3,996	4,003	3,989
End-members (mol %)							
En	34,61	34,05	35,34	24,54	24,59	23,64	34,79
Fs	11,33	10,64	9,14	23,25	26,59	25,28	15,50
Wo	54,05	55,31	55,52	52,20	48,82	51,08	49,71

Chain silicates are comprised mainly by two groups of minerals, namely the pyroxenes (single chain inosilicates) and the amphiboles (double chain inosilicates). The pyroxenes are very common rock-forming minerals found in many different

rocks. The pyroxene formula may, in structural terms, be expressed as M2M1T_2O where M2 and M1 refer to cations in generally distorted and regular octahedral coordination respectively and T to tetrahedrally coordinated cations. Their composition can be described by the general formula: XYZ_2O_6 where the X site is filled by Ca, Na, K, Mn, Fe^{2+} and Mg, the Y site is filled by Al, Cr, Ti, Fe^{3+}, Fe^{2+}, Mn, Mg and Ni and the Z site is filled by Si and Al. Typical pyroxene end-members include minerals such as diopside ($CaMgSi_2O_6$), hedenbergite ($CaFeSi_2O_6$), enstatite ($Mg_2Si_2O_6$) and ferrosilite ($Fe_2Si_2O_6$). Pyroxenes are further subdivided into two separate groups, namely the orthopyroxenes and the clinopyroxenes, according to their crystallographic structure (Deer et al. 1992).

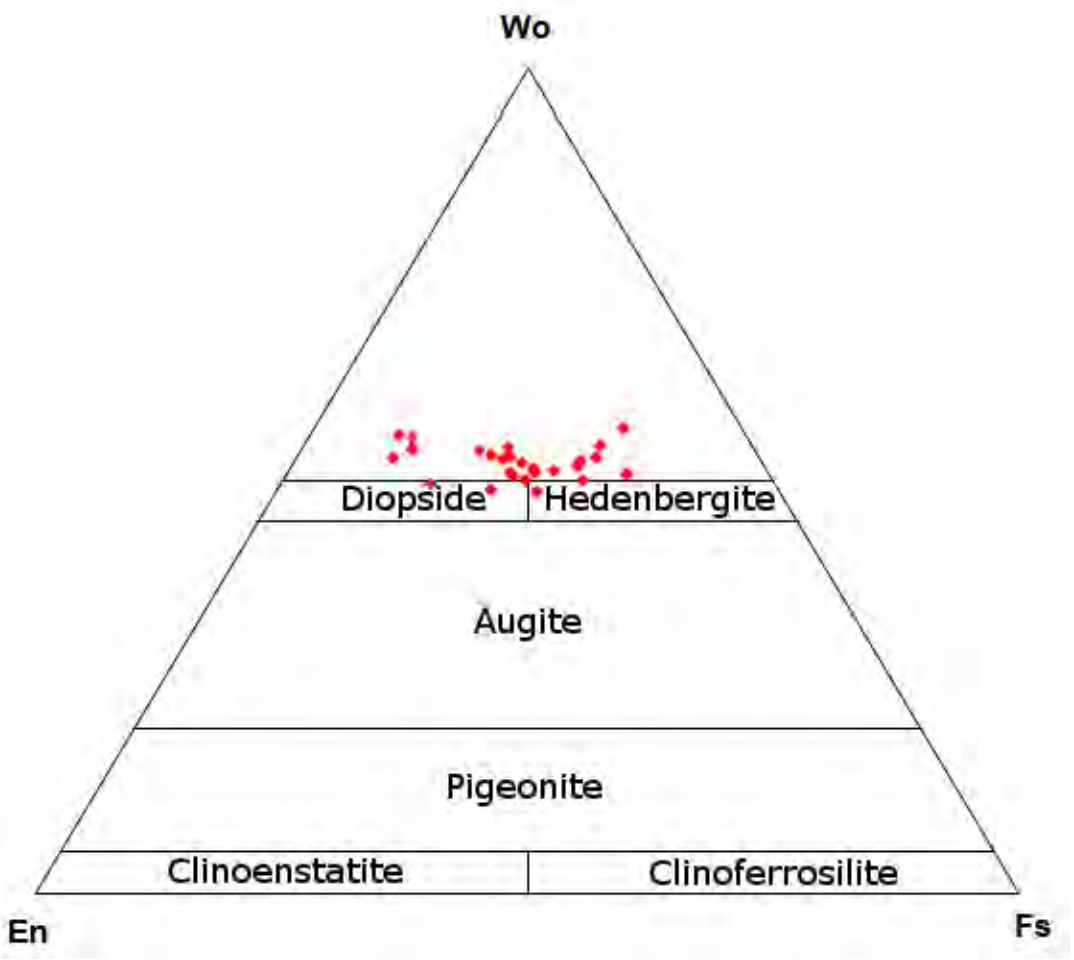

Figure 20: Pyroxene ternary plot based on Morimoto et al. (1988).

The clinopyroxenes found within the Ano Garefi rodingites are lying chemically between the isomorphous series of diopside and hedenbergite which are often found in regional or contact metamorphic rocks. The data from table 5 along with the ternary plot of figure 20 clearly show that the clinopyroxenes are enriched in terms of Ca. As a result the electron probe microanalyses of the Ano Garefi clinopyroxenes tend to gather closer to the wollastonite (Wo) peak in contrast to other pyroxenes from various international references, which in most cases are found below the limit of 50% Wo. The most obvious explanation about this enrichment in Ca is that the rodingite lies in contact with the Ca source, namely the carbonate body and thus the clinopyroxenes were enriched in this specific chemical element.

6.2.4. Chlorite

Selected microanalyses of chlorites from Ano Garefi are presented in Table 6 while their nomenclature according to their chemical composition is graphically shown in Figure 21.

Table 6: Selected microanalyses of chlorites from Ano Garefi.

bdl: below detection limit	1	2	3	4	5	6	7
Oxide weight %							
SiO_2	27,79	27,22	29,22	29,13	29,66	28,54	28,49
TiO_2	0,25	bdl	0,24	0,12	bdl	0,52	bdl
Al_2O_3	17,75	16,96	17,35	17,07	14,88	17,10	18,12
Cr_2O_3	0,31	bdl	bdl	0,14	bdl	0,26	0,19
Fe_2O_3	1,15	0,67	1,83	1,71	0,60	1,63	1,32
FeO	28,99	30,54	26,34	24,62	26,03	25,21	25,37
MnO	0,80	1,68	0,52	1,61	1,46	1,22	1,19
MgO	10,95	11,13	12,56	13,76	14,96	13,53	14,37
Na_2O	0,20	bdl	0,41	0,15	bdl	bdl	bdl
K_2O	0,43	bdl	bdl	bdl	0,53	0,24	bdl
H_2O*	11,16	11,01	11,35	11,37	11,29	11,31	11,47
Total	99,78	99,21	99,82	99,68	99,42	99,56	100,52
Ion distribution based on 28 (O), *) OH is given 16 ignoring H_2O							
Si	5,931	5,921	6,127	6,112	6,277	6,017	5,937
Al	2,069	2,079	1,873	1,888	1,723	1,983	2,063
Al	2,429	2,277	2,450	2,357	2,006	2,290	2,403
Ti	0,040	-	0,037	0,019	-	0,082	-
Cr	0,052	-	-	0,023	-	0,043	0,032
Fe^{3+}	0,184	0,110	0,289	0,269	0,096	0,259	0,207
Fe^{2+}	5,174	5,555	4,618	4,320	4,606	4,444	4,420
Mn	0,144	0,310	0,092	0,286	0,262	0,218	0,210
Mg	3,483	3,608	3,927	4,302	4,720	4,251	4,464
Na	0,168	-	0,336	0,122	-	-	-
K	0,236	-	-	-	0,287	0,128	-
OH*	16,000	16,000	16,000	16,000	16,000	16,000	16,000
Total	35,911	35,859	35,751	35,699	35,978	35,715	35,735

Chlorites are another vast group of minerals with many species due to their chemical differentiation. Their name ascription heavily relies and reflects their chemical composition. They have a layered structure of alternating sheets like the micas. Their structural composition can be described by the general formula: $X_6Z_4O_{10}(OH)_8$, where the X site is filled by Mg, Fe^{2+}, Fe^{3+}, Ni, Mn, Cr^{3+}, Al and Ti while the Z site is filled by Si and Al. However, most chlorite compositions can be represented by the formula: $(R^{2+},R^{3+})_{12}(Si_{8-x}R^{3+})O_{20}(OH)_{16}$, where R^{2+}=Mg, Fe, Mn,

Ni, Zn and R^{3+}=Al, Fe, Cr while x has generally a value of 1 to 3. The composition of the most common chlorites is lying somewhere between that of antigorite's and amesite's with a chemical formula of $Mg_6Si_4O_{10}(OH)_8$ and $(Mg_4Al_2)(Si_2Al_2)O_{10}(OH)_8$ respectively. Mg is very often substituted by Fe either in large or small quantities (Deer et al. 1992, Cristofides and Soldatos 2013).

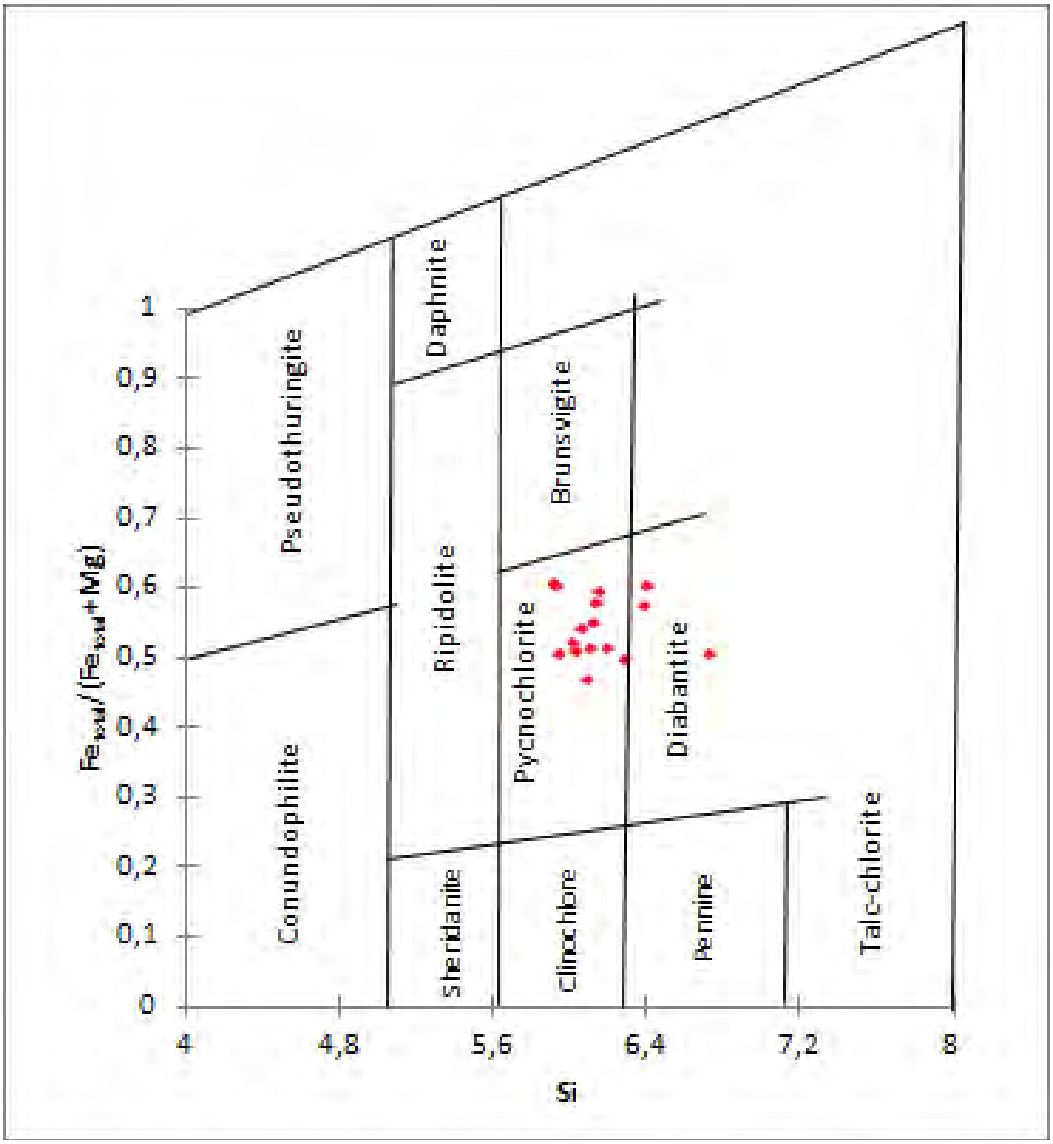

Figure 21: Chlorite plot based on Hey (1954).

Mainly pycnochlorite and secondarily diabantite are the attributed names to the chlorites from Ano Garefi based on the plot shown in Figure 21, which was proposed by Hey (1954) for the chlorite nomenclature.

6.2.5. Combining the results

After presenting the results of the electron probe microanalyses for each mineral it was considered useful to combine some of the data together.

So, the ternary plot Al-Ca-total Fe (Fe^{2+}+Fe^{3+}) was used for the graphic presentation of the electron probe microanalyses of the silicate minerals from Ano Garefi (Figure 22).

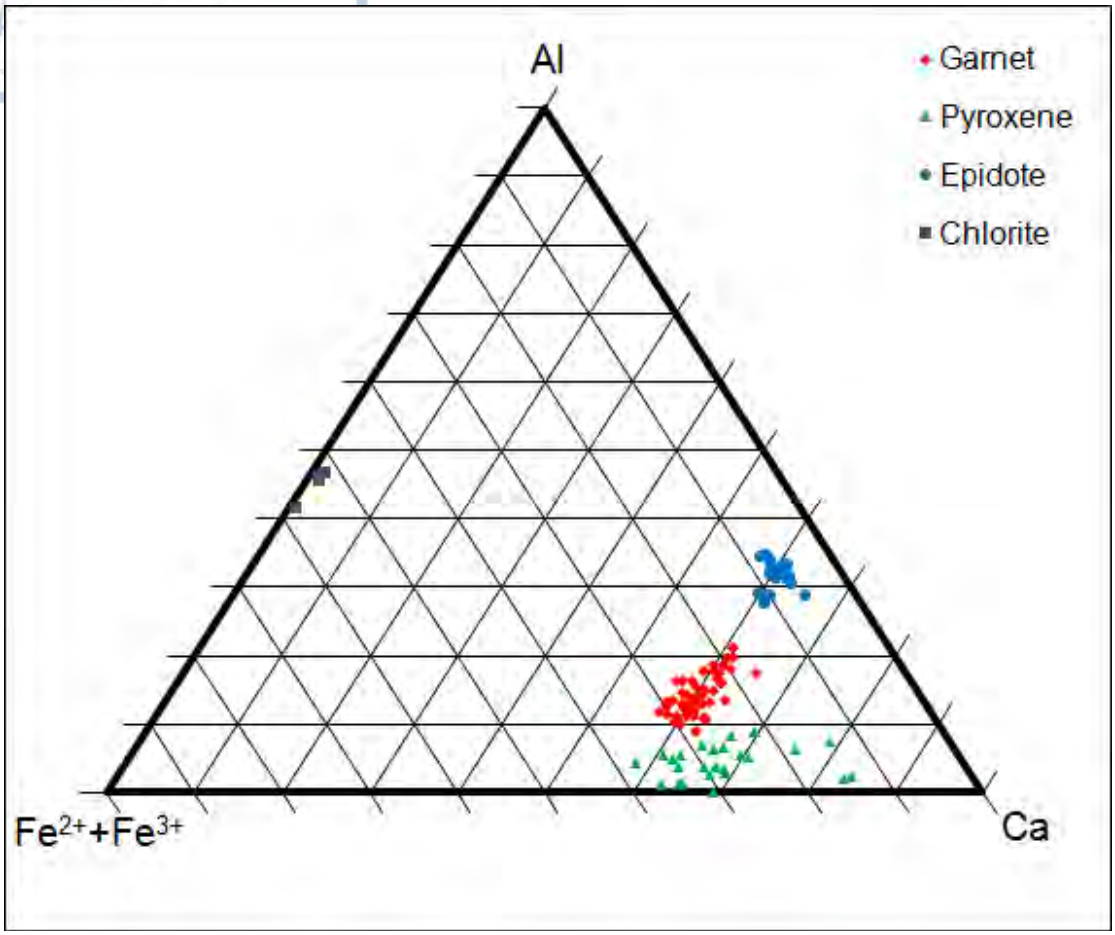

Figure 22: Silicate minerals ternary plot.

The ternary plot of Figure 22 clearly shows that mainly four groups of silicate minerals take part in the formation of the Ano Garefi rodingites. In this plot it is also clear that Ca plays a major role in the formation of rodingites due to the fact that the garnets, the epidotes and the clinopyroxenes are enriched in this element and closer to the specific peak of the plot.

6.3. Chromite

Chromite belongs to the spinel group in which the minerals have the general chemical formula of $R^{2+}R_2^{3+}O_4$ (Deer et al. 1992). The subdivision within this group is based on whether the trivalent cation is Al, Fe or Cr. As a result, the group is subdivided into three series, namely the spinel series with Al as trivalent cation, the magnetite series with Fe as trivalent cation and chromite series with Cr as trivalent cation. Typically chromite is considered to have a chemical formula of $FeCr_2O_4$ but many chemical analyses, gathered through time, actually revealed and showed a more complex crystal in terms of chemical composition. The aforementioned chemical formula is an end-member of the spinel group and found rather rare in nature. Instead, divalent Fe is very often replaced by Mg and thus natural chromites seem to have considerable amounts of this element. Al and even trivalent Fe are two other chemical elements replacing Cr. Mn, Zn and Ti have also been spotted in chromites in small quantities. So a more appropriate chemical formula for chromite should be that of $(Fe^{2+},Mg)(Cr,Al,Fe^{3+})_2O_4$. Ratios like Mg# (100xMg)/(Mg+Fe^{2+}), Cr#

(100xCr)/(Cr+Al) and Fe# (100xFe^{3+})/(Cr+Al+Fe^{3+}), are frequently used when examine minerals of this group in order to extract useful conclusions about their origin.

Selected microanalyses of chromites and ferritchromites from Ano Garefi are presented in Table 7 (the analyses number 6 and number 7 are of ferritchromites while the others are of chromites).

Table 7: Selected microanalyses of chromites from Ano Garefi. Analyses number 6 and number 7 are representative of ferritchromites while the others are of chromites.

bdl: below detection limit	1	2	3	4	5	6	7
Oxide weight %							
SiO_2	0,25	1,00	0,39	1,16	bdl	2,81	0,55
TiO_2	0,37	0,01	0,12	bdl	bdl	bdl	bdl
Al_2O_3	15,73	15,02	16,68	16,89	19,57	2,39	3,53
Cr_2O_3	54,35	51,85	52,10	50,45	50,13	41,57	49,74
Fe_2O_3	0,92	3,51	2,49	2,98	1,28	20,64	13,68
FeO	15,35	15,04	15,38	15,43	15,37	30,37	30,21
MnO	1,56	0,93	1,22	bdl	0,66	1,11	1,73
MgO	11,70	11,54	12,04	12,51	12,30	0,58	0,48
NiO	0,02	1,04	bdl	0,59	0,08	1,13	bdl
Total	100,25	99,94	100,43	100,01	99,40	100,61	99,92
Ion distribution based on 32 (O)							
Si	0,063	0,255	0,097	0,291	-	0,812	0,160
Ti	0,070	0,002	0,023	-	-	-	-
Al	4,711	4,508	4,960	4,995	5,798	0,813	1,221
Cr	10,913	10,435	10,387	10,006	9,959	9,486	11,522
Fe^{3+}	0,176	0,673	0,473	0,563	0,243	4,482	3,017
Fe^{2+}	3,261	3,202	3,245	3,237	3,231	7,332	7,403
Mn	0,337	0,201	0,260	0,000	0,140	0,272	0,429
Mg	4,430	4,378	4,525	4,677	4,607	0,248	0,208
Ni	0,005	0,284	-	0,159	0,022	0,351	-
Total	23,967	23,936	23,970	23,927	24,000	23,797	23,960
Indexes							
$\frac{100xMg}{Mg+Fe^{2+}}$	57,602	57,759	58,241	59,099	58,773	3,275	2,734
$\frac{100xCr}{Cr+Al}$	69,847	69,833	67,680	66,700	63,204	92,105	90,419
$\frac{100xFe^{3+}}{R^{3+}}$	1,114	4,309	2,987	3,615	1,518	30,325	19,144

Unaltered chromites are plotted in the Al-chromite field while altered chromites to ferritchromites are plotted to the Fe-chromite field as shown in the ternary plot of Figure 23.

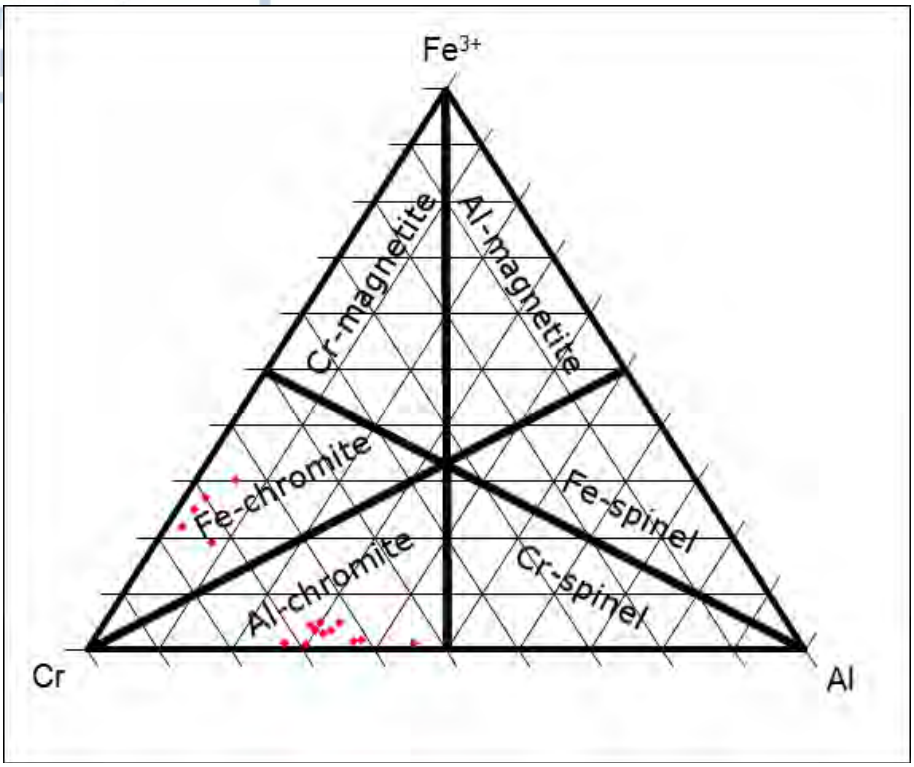

Figure 23: Chromite ternary plot.

Chromites come from the serpentinites. It is possible that the metasomatic process altered them in a high level because some of them are completely disintegrated. The plot in figure 24, based on Irvine and Findlay (1972), indicates that chromites have Cr#>60 and originated from alpine ultrabasic rocks such as dunites.

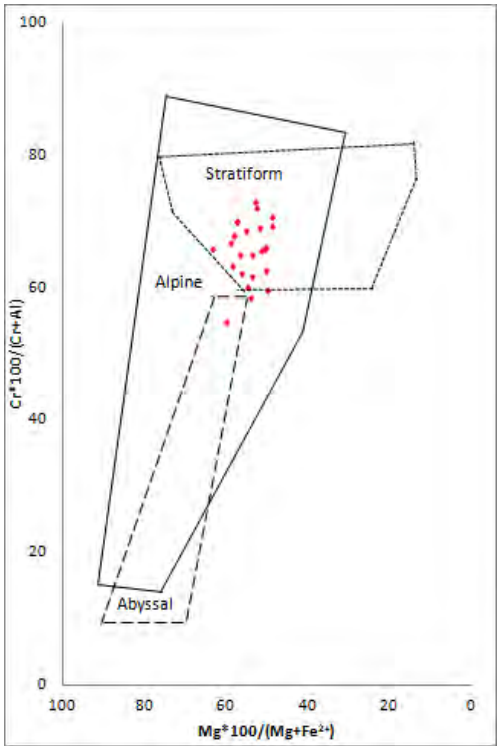

Figure 24: Chromite plot based on Irvine and Findlay (1972).

6.4. Ore minerals

6.4.1. Chalcopyrite

Chalcopyrite is a very important mineral because it is the main ore from which copper can be extracted. It is a chemically composed primarily by copper, iron and sulfur and has a chemical formula of $CuFeS_2$. In most cases it is found in nature having a composition very close to that of its chemical formula but in minor amounts many other elements have also been reported. Some of them are Co, Ni, Mn, Zn and Sb replacing Cu or Fe while As and Se are replacing S. Other elements such as Ag, Au, Pt, Pb, V, Cr, In, Al, Sb and Bi have also been reported (Ramdohr 1980). All the aforementioned chemical elements are not necessarily bind within the structure of chalcopyrite itself but are found as constituents of other minerals intergrown with chalcopyrite in such finely forms that in most cases they are observable only with a high microscope magnification. Such minerals are for example sphalerite which contains Zn, arsenopyrite containing As, stannite containing Sn and many others. Chalcopyrite has a very similar structure with that of sphalerite but there is only limited solid solution between them. Chalcopyrite has the tendency to be oxidized upon exposure on air and water or with slight heating and thus be converted into sulphates of iron and copper and even further into carbonates, hydroxides and oxides. The alteration products, which for example are malachite or azurite, may form pseudomorphs after chalcopyrite (Deer et al. 1992, Ramdohr 1980).

Selected microanalyses of chalcopyrites from Ano Garefi are presented in Table 8 and a ternary plot is shown in Figure 25.

Table 8: Selected electron probe microanalyses of chalcopyrites from Ano Garefi.

bdl: below detection limit	1	2	3	4
Weight %				
S	35,92	35,72	35,63	35,64
Fe	29,88	28,93	31,14	30,56
Co	0,72	0,43	bdl	0,01
Ni	bdl	0,26	0,12	0,62
Cu	33,08	35,08	32,90	32,91
As	0,33	bdl	0,40	0,26
Pb	0,12	0,03	bdl	bdl
Total	100,05	100,45	100,19	100,00
Ion distribution based on 2 (S)				
S	2,000	2,000	2,000	2,000
Fe	0,955	0,930	1,004	0,985
Co	0,022	0,013	-	-
Ni	-	0,008	0,004	0,019
Cu	0,929	0,991	0,932	0,932
As	0,008	-	0,010	0,006
Pb	0,001	-	-	-
Total	3,915	3,942	3,949	3,942

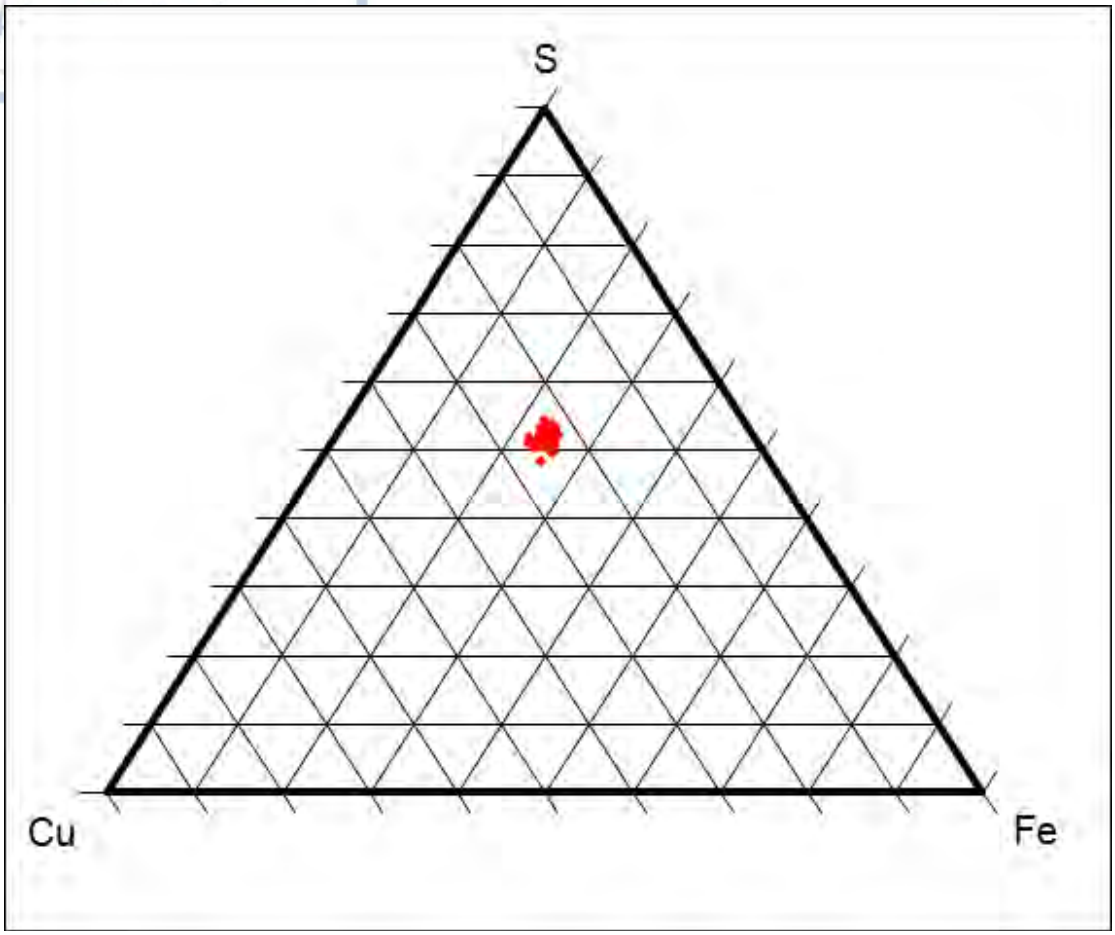

Figure 25: Chalcopyrite ternary plot.

Chalcopyrite from Ano Garefi has a common chemical composition when compared to other chemical analyses conducted in many research papers. Based on 2 S, Fe ranges between 0.827-1.040 with a mean value of 0.931 while Cu ranges between 0.824-1.081 with a mean value of 0.944. The other chemical elements are found in trace quantities or below the detection limit for the analytical method used. Therefore, the mean chemical composition of chalcopyrite is $Cu_{0.94}Fe_{0.93}Co_{0.01}S_2$.

6.4.2. Pentlandite

Pentlandite is a sulfide of Fe and Ni and is characterized by the $(Fe,Ni)_9S_8$ chemical formula. Co is another very common chemical element participating in the formation of pentlandite by replacing Ni. The extent of replacement varies a lot and may be complete or in small amounts (Ramdohr 1980).

Selected microanalyses of pentlandites from Ano Garefi are presented in Table 9 and a ternary plot is shown in Figure 26.

Although pentlandite is found in minor amounts in the Ano Garefi rodingites, it is an interesting find due to the fact that it seems to be enriched in terms of Co according to the results from the electron probe microanalyses that were conducted. As mentioned before pentlandite is characterized by the $(Fe,Ni)_9S_8$ chemical formula but Co may replace the other metals partly or even totally. Based on 8 S, Co ranges between 4.912-5.961 with a mean value of 5.312. Fe ranges between 0.911-1.580 with a mean value of 1.188, Ni ranges between 1.604-2.682 with a mean value of 2.008 while Cu ranges between 0.000-0.155 with a mean value of 0.041.

Table 9: Selected microanalyses of pentlandites from Ano Garefi.

bdl: below detection limit	1	2	3	4	5	6
Weight %						
S	32,84	33,06	33,93	33,67	31,92	33,04
Fe	10,55	11,37	8,70	9,09	9,28	6,72
Co	41,65	38,37	39,26	40,98	38,49	45,25
Ni	15,19	16,99	17,67	16,82	19,58	13,58
Cu	0,27	0,31	1,30	0,24	0,35	0,80
As	bdl	bdl	bdl	bdl	0,64	0,61
Total	100,49	100,11	100,86	100,79	100,26	100,00
Ion distribution based on 8 (S)						
S	8,000	8,000	8,000	8,000	8,000	8,000
Fe	1,475	1,580	1,178	1,240	1,336	0,934
Co	5,521	5,052	5,037	5,297	5,249	5,961
Ni	2,022	2,246	2,276	2,183	2,682	1,796
Cu	0,033	0,038	0,155	0,028	0,044	0,098
As	-	-	-	-	0,069	0,063
Total	17,051	16,917	16,645	16,748	17,380	16,853

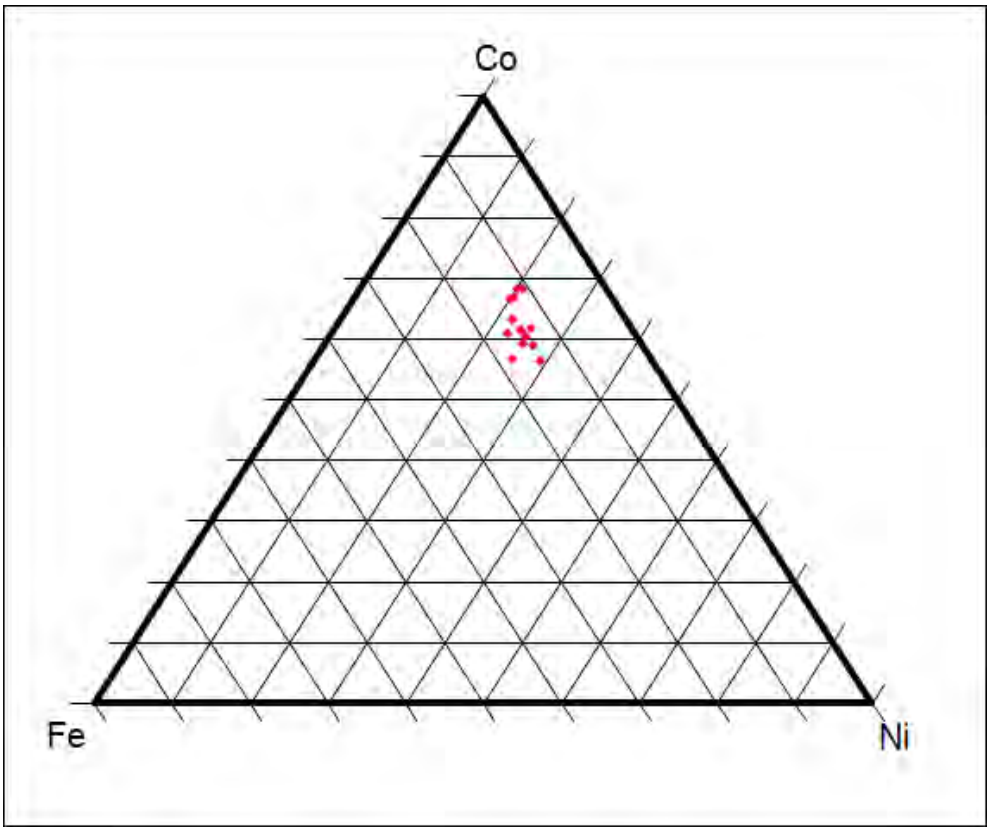

Figure 26: Pentlandite ternary plot.

Other elements such as As or Pb are found only in trace amounts. Therefore, the chemical formula $(Co_{5.31}Fe_{1.19}Ni_{2.01}Cu_{0.04})S_8$ can be given for the studied pentlandite.

Stumpfl and Clark (1964) in their report, found pure cobalt pentlandite in the Vauze copper mine with values of 66.6% Co, 0.1% Ni, 1.3% Fe, 0.3% Cu and 31.7% Scounakis et al. (1982) in their investigation, report a Co-pentlandite in the ophiolite complex of Pindos found within pyrrhotite ore bodies in gabbros and near the contact with serpentinites. The chemical composition of their Co-pentlandite corresponds to the formula: $Co_{8.59}Fe_{0.59}S_8$ and the Ni and Cu contents are less than 0.1wt%. In another investigation, Harney and Merkle (1992) report Co-rich pentlandites found in the eastern Bushveld Complex. They claim that hydrothermal processes played an important role in changing the sulfide mineralogy and composition and led to an increase in Co content on the pentlandite grains by substituting Fe. So after all, the pentlandites from Ano Garefi are not exquisite but they are not so common as well.

6.4.3. Sphalerite

The chemical formula of sphalerite is ZnS but it is rather rare to be found naturally in its pure form because practically always Zn is substituted by Fe. Other substituting chemical elements of Zn are often Mn and Cd and sometimes Ga, In, Tl and Hg in small amounts (Ramdohr 1980). The aforementioned chemical elements although they are found in small or trace amounts in sphalerite they constitute a valuable resource because many new technological discoveries heavily rely on those metals for their manufacture. Due to the fact that these metals are not so easy-found in nature, when detected in sphalerite they can increase and even multiply its value and thus make it worth for mining in cases where otherwise it would be a waste of money and time to extract it due to its low grade (Deer et al. 1992, Ramdohr 1980).

Selected microanalyses of sphalerites from Ano Garefi are presented in Table 10 and a ternary plot is shown in Figure 27.

Table 10: Selected microanalyses of sphalerites from Ano Garefi.

bdl: below detection limit	1	2	3	4	5	6	7
Weight %							
S	34,24	33,14	34,45	33,98	33,71	33,94	33,71
Mn	bdl	0,20	bdl	0,61	bdl	bdl	0,79
Fe	2,80	3,10	2,55	2,16	2,44	1,28	2,43
Zn	62,12	63,18	63,29	62,14	63,65	63,45	61,35
As	bdl	0,26	bdl	0,64	0,40	0,17	0,33
Cd	0,99	0,12	bdl	0,46	0,12	1,22	1,40
Total	100,15	100,00	100,29	99,99	100,32	100,06	100,01
Ion distribution based on 1 (S)							
S	1,000	1,000	1,000	1,000	1,000	1,000	1,000
Mn	-	0,004	-	0,010	-	-	0,014
Fe	0,047	0,054	0,043	0,036	0,042	0,022	0,041
Zn	0,890	0,935	0,901	0,897	0,926	0,917	0,892
As	0,000	0,003	-	0,008	0,005	0,002	0,004
Cd	0,008	0,001	-	0,004	0,001	0,010	0,012
Total	1,945	1,996	1,943	1,956	1,974	1,951	1,964

Sphalerite in study is characterized by relatively low iron contents (1.28-3.10 wt% Fe), while Cd values are up to 1.40wt%. The mean chemical composition of the mineral is $Zn_{0.90}Fe_{0.04}Cd_{0.01}S$.

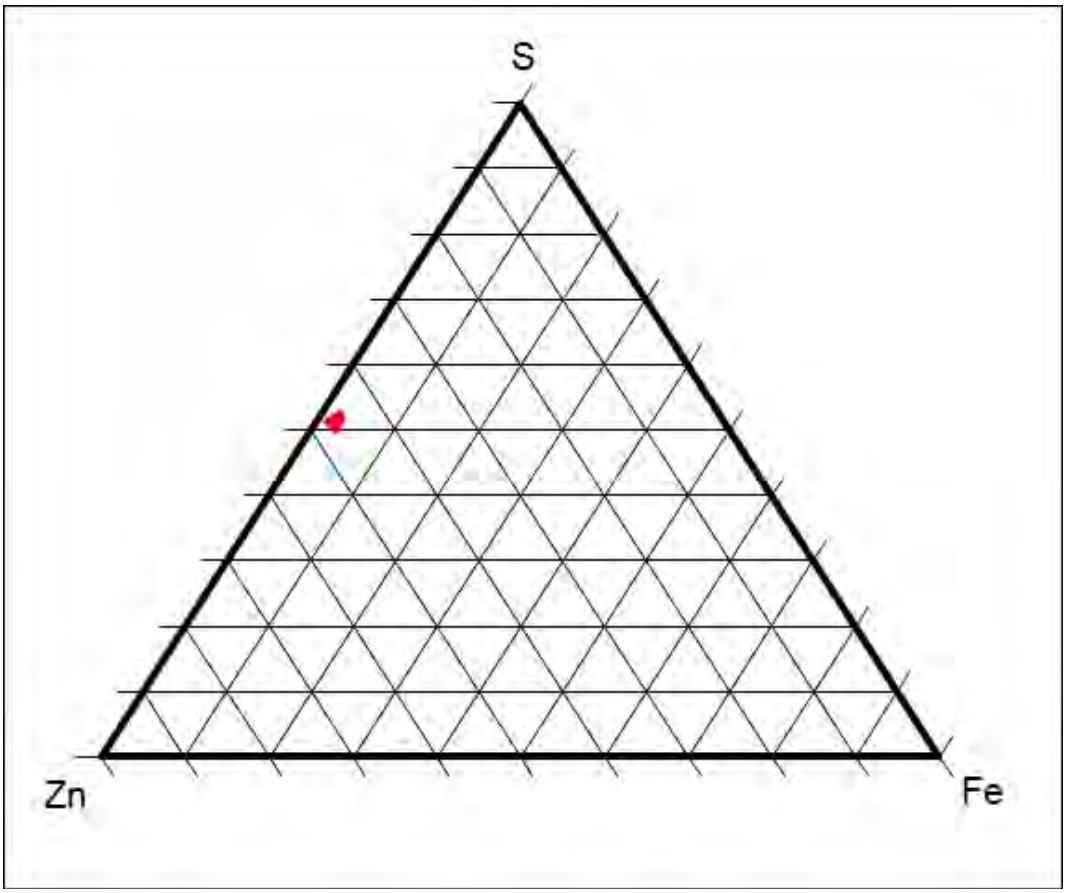

Figure 27: Sphalerite ternary plot.

Based on 1 S, Zn atoms ranges between 0.860-0.935 with a mean value of 0.896 while Fe ranges between 0.022-0.054 with a mean value of 0.039. The other elements are in minor quantities.

7. Discussion

Considering the metasomatic process, the mineral paragenesis is not a standard thing occurring every time as the exact same percentage of the same minerals but it is very variable and depends on a high level on local factors such as the geotectonic environment and the presence or not of the appropriate sources which will provide the necessary elements for the rodingite formation. The differentiation in mineral assemblages can be highlighted by some examples taken from various scientific papers about rodingites. So, Schandl et al. (1989) described rodingites with diopside + garnet + tremolite + vesuvianite or with diopside + epidote + titanite or diopside + garnet + prehnite + chlorite. Schandl et al. (1989) were also the first to categorize the rodingites according to their mineral assemblages into three groups, each one representing a different but successive stage of metasomatic alteration. The earliest alteration of the protolith gives as a product rodingites rich in epidote group minerals. During the second and more advanced stage of alteration, grossular and prehnite rich rodingites are formed. In the final and most extensive stage of alteration diopside rich rodingites are formed. Hatzipanagiotou and Tsikouras (2001) described rodingites with garnet + vesuvianite + diopside + epidote + calcite + prehnite or epidote + calcite + diopside + prehnite ± chlorite ± albite. Murzin and Shanina (2007), a case study with gold mineralization, described rodingites with an initial chlorite + andradite + diopside paragenesis cross cutted by later stage veins and veinlets of diopside and calcite. Normand and Williams-Jones (2007) described rodingites with hydrogrossular + clinopyroxene + zoisite + chlorite + prehnite + vesuvianite + wollastonite. Koutsovitis et al. (2013) referred on two types of rodingites based on their mineral assemblages. The first type consists of prehnite + clinopyroxene + amphibole + chlorite ± hydrogarnet ± pumpellyite ± white mica ± calcite with rare albite, magnetite, ilmenite and titanite. The second type consists of hydrogarnet ± garnet + clinopyroxene + chlorite ± vesuvianite with rare prehnite, pumpellyite, amphibole, calcite, magnetite, ilmenite, spinel and titanite. Recently, Tsikouras et al. (2013) described rodingites consisting of garnet + chlorite + diopside + prehnite + tremolite ± vesuvianite ± epidote and epidote + clinozoisite + prehnite + tremolite.

According to Bach and Klein (2008) rodingites have been found in a range of tectonic settings. For example they have been found in seafloor spreading centers (Hekinian et al. 1993), in rifted continental margins (Beard et al. 2002), in ophiolites (Austrheim and Prestvik 2008), in greenstone belts (Schandl et al. 1989, O'Hanley et al. 1992, Normand and Williams-Jones 2007), in alpine settings (Li et al. 2004, Murzin and Shanina 2007) and in suprasubduction zones (Li et al. 2007, Fukuyama et al. 2014).

The rodingite's mechanism of formation is yet unclear and it is a matter of debate amongst geoscientists. Many theories have been proposed in order to interpret their creation but they only apply on a local scale. It is possible that the rodingites can be created in more than one ways. Some believe that the rodingitization happens when Ca-rich and Si-poor hydrothermal fluids, generated and originated by the serpentinization of the neighboring ultramafic rocks, infiltrate and metasomatize the protoliths (Schandl et al. 1989, Koutsovitis et al. 2013). Others claim that rodingites are the product of Si, Na, K and Mg depletion during or after serpentinization (Hatzipanagiotou and Tsikouras 2001, Pomonis et al. 2008). A third but not so widespread opinion about the formation of the rodingites is that they are the product of an autometasomatic process which happens when postmagmatic fluids are released from a cooling basic magma (Zharikov et al. 2007). Of course, all of the

aforementioned theories may be hold and lead to rodingite production depending on the geotectonic environment and under different physicochemical conditions.

Murzin and Shanina (2007), based on isotope calculation, suggested that the rodingites in the Karabash ultramafic massif in the Urals are of metamorphic origin. They were formed from the water released from the serpentinites during their dehydration, enriched in components from the basic and ultrabasic magmatic rocks and at a final stage from marine carbon. The temperature of formation was 420-470^{o}C and the pressure 2-3kbar during the initial stages. The aforementioned range of temperatures and pressures are typical of rodingite formation. At a later stage the temperature drops at 230-310^{o}C and the pressure at 0.5-1kbar while an increase in CO_2 is thought possible based on the high concentration in fluid inclusions.

Normand and Williams-Jones (2007) suggest that the rodingitization process took place in three separate episodes during the thrusting of the ophiolites onto the Laurentian margin. The temperatures and pressures of the first and second episodes were 290-360^{o}C/2.5-4.5kbar and 325-400^{o}C/3kbar respectively. The fluids were moderately to strongly saline. The third episode indicates significantly lower temperatures and salinity. The methane content found in the fluid inclusions of these rodingites suggests that the rodingite forming fluid originates from the serpentinites.

According to Koutsovitis et al. (2013), the rodingites from East Orthis were formed in an intraoceanic subduction system. The rodingitization process occurred in three successive stages during the exhumation of the mafic and ultramafic mantle wedge rocks in a forearc tectonic environment along a serpentinitic subduction channel, which developed near the slab. The incorporation of the mafic rocks to the subduction channel probably resulted after entraining a directed mantle flow towards the slab. All three rodingitization stages were estimated to have occurred under relatively moderate temperature (300-400^{o}C) and pressure (3-6kbar).

Regarding the Ano Garefi case, field investigation combined with optical observations from a transmitted and a reflected light microscope along with electron probe microanalyses conducted by a SEM allow a brief interpretation about the possible geologic process that may have lead to the rodingite formation and the extraction of some conclusions.

It seems possible that, sometime during the past, small or big carbonate bodies were tectonically entrapped and enclosed inside the serpentinites. This enclosure could have happened during one of the many orogenic movements with a general direction from east to west that formed over time the Greek tectonic landscape and created continuous thrust faults, thrust sheets and in general nappe pile and nappe stacking. Tectonic indexes imprinted onto the serpentinites along with the carbonate bodies and especially near their contact were observed during the field investigation. These indexes support enhance the opinion of intense deformation during a tectonic thrust event. Hydrothermal fluids, circulating through the surrounding basic and ultrabasic rocks, gradually got enriched in the necessary chemical elements for the rodingite formation. This enrichment could be the result of the depletion of the neighboring rocks. More specifically, the source of Ca could be the carbonate bodies while the other elements such as Fe, Mg, Ni and Co derived from ultrabasics. Al present in the silicate minerals along with Cu and Zn, necessary for the chalcopyrite and sphalerite formation, may originate from the dolerites found in the area. The deposition of the hydrothermal fluids and the rodingite formation probably took place between tectonically weakened zones inside the serpentinites and in contact with the carbonate bodies.

The reaction zone is clearly shown in figure 8. A mineral assemblage differentiation along a line, starting from the unaltered carbonate body, through the rodingite and finishing inside the serpentinite is thought quite possible. If such a research, by taking and analyzing samples along this line is carried out, it might reveal some separate stages during the metasomatic process and also clarify the physicochemical conditions under which the rodingites were formed.

At the end, a suggested research, triggered by the lack of evidence of what caused the ore mineral deposition, could be a more detailed investigation of when and under which circumstances ore mineralization of any kind is deposited inside the rodingites.

8. Conclusions

The study of the rodingites from Ano Garefi revealed the following:

1. The Ano Garefi rodingites occur as pods, veins and blocks enclosed in serpentinites and usually adjacent to small or large tectonically included carbonate bodies. Macroscopically and in hand specimens, they have a pale green-brown color, while their mineral constituents are medium- to coarse-grained.

2. The identified mineral assemblages consist of calcite + garnet + epidote + clinopyroxene + chlorite ± chromite + chalcopyrite ± pentlandite ± sphalerite.

3. Garnets chemically belong to the ugrandite series with andradite as the dominant end-member. The rims of the garnet crystals are usually overgrown by a thin epidote crust. Clinopyroxenes are of diopside-hedenbergite composition. Additionally, wollastonite compositions were found as a result of enrichment in terms of Ca due to the close contact between the rodingites and the carbonate bodies. Chlorite has a pycnochlorite composition.

4. Chromite is a relic mineral from serpentinite protolith and occurs as partly altered to ferritchromite fractured clasts showing evidence of tectonic deformation.

5. The ore minerals chalcopyrite with minor pentlandite and sphalerite form local segregations filling the interstices between the gangue minerals and account for about 5% by volume of the rodingite body. Chalcopyrite, pentlandite, and sphalerite, have the following mean chemical compositions: $Cu_{0.94}Fe_{0.93}Co_{0.01}S_2$, $(Co_{5.31}Fe_{1.19}Ni_{2.01}Cu_{0.04})S_8$ and $Zn_{0.90}Fe_{0.04}Cd_{0.01}S$, respectively.

6. Textural features and mineral associations of the copper bearing rodingites in study, denote that their formation can be attributed to a metasomatic process by means of hydrothermal fluids. These fluids were enriched in the necessary chemical elements by the depletion of the surrounding rocks and circulated through tectonically weakened zones. The reaction zone occurs between carbonate bodies and serpentinites. The carbonate bodies are the main source of Ca while serpentinites are the source of Fe and Mg. Dolerites, associated with the serpentinites, are the most likely source for Al and Cu.

9. Περίληψη

Ο στόχος της εργασίας αυτής ήταν να μελετηθεί η ορυκτολογική παραγένεση των ροδινγκιτών από το Άνω Γαρέφι στην περιοχή της Αριδαίας (Βόρεια Ελλάδα) και να πιστοποιηθούν οι συνθήκες κάτω από τις οποίες σχηματίστηκαν αυτά τα πετρώματα και κυρίως να διερευνηθεί γενετικά η όχι και τόσο συχνή χαλκούχα μεταλλοφορία που συνοδεύει τους ροδινγκίτες σε σχέση με τη διαδικασία της ροδινγκιτίωσης. Η περιοχή μελέτης είναι το ορεινό ανάγλυφο πάνω από το χωριό του Άνω Γαρεφίου που γεωτεκτονικά ανήκει στην υποζώνη της Αλμωπίας της ζώνης Αξιού. Οι ροδινγκίτες στο Άνω Γαρέφι έχουν μορφή λοβών, φλεβών ή μεγάλων ογκόλιθων και είναι έγκλειστοι μέσα στους σερπεντινίτες και συνήθως βρίσκονται σε επαφή με κάποιο μικρό ή μεγάλο, τεκτονικώς εγκλεισμένο, ανθρακικό σώμα. Μακροσκοπικά οι ροδινγκίτες εμφανίζουν ένα απαλό καφεπράσινο χρώμα και τα ορυκτά συστατικά είναι μεσόκοκκα έως αδρόκοκκα. Οι ορυκτολογικές συγκεντρώσεις που αναγνωρίστηκαν αποτελούνται από ασβεστίτη + γρανάτη + επίδοτο + κλινοπυρόξενο + χλωρίτη ± χρωμίτη + χαλκοπυρίτη ± πεντλανδίτη ± σφαλερίτη. Ο ασβεστίτης εμφανίζεται με τη μορφή τοπικών κλαστών, με τη μορφή φλεβών ή ακόμα και με τη μορφή μεγάλων κρυστάλλων που εγκλείουν άλλα πυριτικά ορυκτά. Οι γρανάτες εμφανίζονται συχνά καλά κρυσταλλωμένοι και εμφανίζουν χρώματα πόλωσης και είναι ανισότροποι. Μια ζωνώδης κατανομή και μια χημική διαφοροποίηση από τον πυρήνα προς το περιθώριο μπορεί να βρεθεί στους περισσότερους κρυστάλλους γρανατών. Χημικώς, ανήκουν στη σειρά των ουγρανδιτών με τον ανδραδίτη να είναι το επικρατών ακραίο μέλος Η περιφέρεια των γρανατών καταλαμβάνεται συνήθως από μια λεπτή κρούστα από επίδοτο. Το επίδοτο σχηματίζει επίσης ξεχωριστούς ιδιόμορφους και πρισματικούς κρυστάλλους. Οι κλινοπυρόξενοι που βρέθηκαν στους ροδινγκίτες του Άνω Γαρεφίου έχουν σύσταση μεταξύ διοψιδίου-εδενβεργίτη. Επιπλέον, συστάσεις βολλαστονίτη εντοπίστηκαν ως αποτέλεσμα του εμπλουτισμού σε Ca εξαιτίας της στενής επαφής μεταξύ των ροδινγκιτών και των ανθρακικών σωμάτων. Ο χλωρίτης εντοπίζεται με τη μορφή μικρών ανοιχτοπράσινων νιφάδων και βρίσκεται μεταξύ των άλλων ορυκτών και έχει σύσταση πυκνοχλωρίτη. Ο χρωμίτης είναι ένα υπολειμματικό ορυκτό από τους σερπεντινικούς πρωτόλιθους και έχει τη μορφή μερικώς αλλοιωμένων σε σιδηροχρωμίτη διαρρηγμένων κλαστών που δείχνουν στοιχεία τεκτονικής καταπόνησης. Τα μεταλλικά ορυκτά, αποτελούνται κυρίως από χαλκοπυρίτη με μικρές εμφανίσεις πεντλανδίτη και σφαλερίτη που βρίσκονται ως τοπικά συσσωματώματα γεμίζοντας τα διάκενα μεταξύ των στείρων ορυκτών. Τα σουλφίδια καταλαμβάνουν το 5% του όγκου του ροδινγκίτη. Ο χαλκοπυρίτης από το Άνω Γαρέφι έχει τυπική χημική σύσταση. Οι ατομικές αναλογίες σε Cu και Fe, με βάση 2 S, κυμαίνονται μεταξύ 0.824-1.081 (μέση τιμή 0.944) και 0.827-1.040 (μέση τιμή 0.931), αντίστοιχα. Ο πεντλανδίτης αποτελεί κοβαλτιούχο ποικιλία του ορυκτού με ατομικές αναλογίες σε Co, Fe και Ni, με βάση 8 S, να κυμαίνονται στα όρια μεταξύ 4.912-5.961 (μέση τιμή 5.312), 0.911-1.580 (μέση τιμή 1.188) και 1.604-2.682 (μέση τιμή 2.008), αντίστοιχα. Ο σφαλερίτης χαρακτηρίζεται από σχετικά χαμηλές περιεκτικότητες σε Fe. Με βάση 1 S, ο Zn κυμαίνεται μεταξύ 0.860-0935 με μια μέση τιμή 0.896 ενώ ο Fe κυμαίνεται μεταξύ 0.022-0.054 με μια μέση τιμή 0.039. Ιστολογικά χαρακτηριστικά και σχέσεις μεταξύ

των ορυκτών στους εξεταζόμενους χαλκούχους ροδινγκίτες, υποδηλώνουν ότι ο σχηματισμός τους μπορεί να αποδοθεί σε μια μετασωματική διαδικασία μέσω υδροθερμικών ρευστών. Αυτά τα ρευστά ήταν εμπλουτισμένα στα απαραίτητα χημικά στοιχεία από την έκπλυση των περιβαλλόντων πετρωμάτων και κυκλοφορούσαν μέσω ασθενών τεκτονικών ζωνών. Η ζώνη αντίδρασης βρίσκεται μεταξύ των ανθρακικών σωμάτων και των σερπεντινιτών. Τα ανθρακικά σώματα είναι η κύρια πηγή Ca ενώ οι σερπεντινίτες είναι η πηγή του Fe και του Mg. Οι δολερίτες, που σχετίζονται με τους σερπεντινίτες, είναι η πιο πιθανή πηγή για το Al και τον Cu.

10. References

Armbruster T., Bonazzi P., Akasaka M., Bermanec V., Chopin C., Giere R., Heuss-Assbichler S., Liebscher A., Menchetti S., Pan Y. and Pasero M. (2006). Recommended nomenclature of epidote-group minerals. European Journal of Mineralogy, 18, 551-567.

Austrheim H. and Prestvik T. (2008). Rodingitization and hydration of the oceanic lithosphere as developed in the Leka ophiolite, north–central Norway. Lithos, 104, 177-198.

Bach W. and Klein F. (2008). The petrology of seafloor rodingites. Insights from geochemical reaction path modeling. Lithos, 112, 103-117.

Beard J., Fullagar P. and Sinha K. (2002). Gabbroic pegmatite intrusions, Iberia Abyssal Plain, ODP Leg 173, Site 1070 magmatism during a transition from non-volcanic rifting to sea-floor spreading. Journal of Petrology, 43 (5), 885-905.

Beeson M. and Jackson E. (1969). Chemical composition of altered chromites from the Stillwater Complex, Montana. The American Mineralogist, 54, 1084-1100.

Bell J., Clarke E. and Marshall P. (1911). The geology of the Dun mountain subdivision, Nelson. New Zealand Geological Survey, 12 (new series).

Christofides G. and Soldatos T. (2013). Optical mineralogy (in Greek). Giachoudis press, 394p.

Deer W.A., Howie R.A. and Zussman J. (1992). An introduction to the rock forming minerals 2nd edition. Addison Wesley Longman Limited, 696p.

Fukuyama M., Ogasawara M., Dunkley D., Wang K.-L., Lee D.-C., Hokada T., Maki K., Hirata T. and Kon Y. (2014). The formation of rodingite in the Nagasaki metamorphic rocks at Nomo peninsula, Kyushu, Japan. Zircon U-Pb and Hf isotopes and trace element evidence. Island Arc, 23, 281-298.

Galeos A., Karfakis I. and Fotiadis A. (1979-1983 and 1997). Geological map of Greece 1:50000, Promahi sheet. Institute of Geology and Mineral Exploration.

Harney D. and Merkle R. (1992). Sulfide mineralogy at the main magnetite layer, upper zone, eastern Bushveld Complex and the effect of hydrothermal processes on pentlandite composition. European Journal of Mineralogy, 4, 557-569.

Hatzipanagiotou K. and Tsikouras B. (2001). Rodingite formation from diorite in the Samothraki ophiolite, NE Aegean, Greece. Geological Journal, 36, 93-109.

Hekinian R., Bideau D., Francheteau J., Cheminee J.-L., Armijo R., Lonsdale P., and Blum N. (1993). Petrology of the east Pacific rise crust and upper mantle exposed in Hess Deep (eastern equatorial Pacific). Journal of Geophysical Research, 98 (B5), 8069-8094.

Hey M. (1954). A new review of the chlorites. The Mineralogical Magazine, 30 (224).

Irvine T.N. and Findlay T.C. (1972). The ancient oceanic lithosphere. Alpine type peridotite with particular reference to the Bay of Islands complex. Publications of the Earth Physics Branch, Canadian Department of Energy, Mines and Resources, Canadian contribution number 8 to the geodynamics project, 97-128.

Katrivanos E., Kilias A. and Mountrakis D. (2013). Kinematics of deformation and structural evolution of the Paikon massif (central Macedonia, Greece). A Pelagonian tectonic window?. New Yearbook for Geology and Paleontology (in German), 269 (2), 149-171.

Kilias A., Frisch W., Avgerinas A., Dunkl I., Falalakis G. and Gawlick H.-J. (2010). Alpine architecture and kinematics of deformation of the northern Pelagonian nappe pile in the Hellenides. Austrian Journal of Earth Sciences, 103 (1), 4-28.

Koutsovitis P., Magganas A., Pomonis P. and Ntaflos T. (2013). Subduction-related rodingites from east Ohtris, Greece: Mineral reactions and physicochemical conditions of formation. Lithos, 172/173, 139-157.

Li X.-P., Rahn M. and Bucher K. (2004). Metamorphic processes in rodingites of the Zermatt-Saas ophiolites. International Geology Review, 46 (1), 28-51.

Li X.-P., Zhang L., Wei C., Ai Y. and Chen J. (2007). Petrology of rodingite derived from eclogite in western Tianshan, China. Journal of Metamorphic Geology, 25, 363-382.

Mercier J. (1968). Geological study of the internal Hellenides in central Macedonia. Contribution to the study of metamorphism and evolution of magmatism in internal Hellenides (in French). Geological Annals of Greece (in French), 20, 792p.

Merlini A., Grieco G., Diella V. (2009). Ferritchromite and chromian-chlorite formation in melange-hosted Kalkan chromitite (Southern Urals, Russia). The American Mineralogist, 94 (10), 1459-1467.

Michailidis K. (1990). Zoned chromites with high Mn-contents in the Fe-Ni-Cr-laterite ore deposits from the Edessa area in Northern Greece. Mineralium Deposita, 25 (3), 190-197.

Migiros G. and Galeos A. (1990). Tectonic and stratigraphic significance of the Ano Garefi ophiolite rocks, northern Greece. Proceedings of the 'Troodos 1987' symposium, 279-284.

Morimoto N., Fabries J., Ferguson A.K., Ginzburg I.V., Ross M., Seifert F.A., Zussman J., Aoki K. and Gottardi G. (1988). Nomenclature of pyroxenes. American Mineralogist, 73, 1123-1133.

Mountrakis D. (2010). Geology and geotectonic evolution of Greece (in Greek). University studio press, 373p.

Murzin V.V. and Shanina S.N. (2007). Fluid regime and origin of gold bearing rodingites from the Karabash alpine type ultrabasic massif, southern Ural (in Russian). Geochemistry (in Russian), 10, 1085-1099.

Murzin V.V., Oydup C.K. and Varlamov D.A. (2009). A new finding of Cu-Au alloy in association with rodingite minerals in the Kaa-Khem ophiolitic belt, Tuva (in Russian). Proceedings of the Russian Mineralogical Society (in Russian), 6, 85-98.

Normand C. and Williams-Jones A. (2007). Physicochemical conditions and timing of rodingite formation. Evidence from rodingite-hosted fluid inclusions in the JM Asbestos mine, Asbestos, Quebec. Geochemical Transactions, 8 (11).

O'Hanley D., Schandl E. and Wicks F. (1992). The origin of rodingites from Cassiar, British Columbia, and their use to estimate T and P (H_2O) during serpentinization. Geochimica et Cosmochimica Acta, 56, 97-108.

O'Hanley D. (1996). Serpentinites: Records of tectonic and petrological history. Oxford university press, 277p.

Pomonis P., Tsikouras B., Karipi S. and Hatzipanagioutou K. (2008). Rodingite formation in ultramafic rocks from the Koziakas ophiolite, western Thessaly, Greece. Conditions of metasomatic alteration, geochemical exchanges and T-X(CO_2) evolutionary path. The Canadian Mineralogist, 46, 569-581.

Ramdohr P. (1980). The ore minerals and their intergrowths. 2nd edition, Pergamon press.

Saumur B.-M. and Hattori K. (2013). Zoned Cr-spinel and ferritchromite alteration in forearc mantle serpentinites of the Rio San Juan Complex, Dominican Republic. Mineralogical Magazine, 77 (1), 117-136.

Schandl E., O'Hanley D. and Wicks F. (1989). Rodingites in serpentinized ultramafic rocks of the Abitibi greenstone belt, Ontario. The Canadian Mineralogist, 27, 579-591.

Scounakis S., Sideris C. and Economou M. (1982). A new natural occurrence of Co_9S_8 in pyrrhotite ore from the ophiolite complex of Pindos, Greece. New Yearbook for Mineralogy (in German), 5, 169-174.

Spangenberg K. (1943). The chromite beds of Tampadel in Zobten (in German). Journal of Practical Geology (in German), 5, 13-35.

Stumpfl E. and Clark A. (1964). A natural occurrence of Co_9S_8, identified by X-ray microanalysis. New Yearbook for Mineralogy (in German), 240-245.

Tsikouras B., Karipi S. and Hatzipanagioutou K. (2013). Evolution of rodingites along stratigraphic depth in the Iti and Kallidromon ophiolites. Lithos, 175/176, 16-29.

Ulmer C. (1974). Alteration of chromite during serpentinization in the Pennsylvania-Maryland district. The American Mineralogist, 59, 1236-1241.

Zharikov V.A., Pertsev N.N., Rusinov V.L., Callegari E. and Fettes D.J. (2007). Metasomatism and metasomatic rocks. Recommendations by the IUGS subcommission on the systematics of metamorphic rocks, web version 01.02.07.